

# Physical Properties of Wolf-Rayet Stars

PAUL A. CROWTHER

*Department of Physics & Astronomy, University of Sheffield, Hounsfield Road, Sheffield, S3 7RH, United Kingdom, email: Paul.Crowther@sheffield.ac.uk*

**Key Words** stars: Wolf-Rayet; stars: fundamental parameters; stars: evolution; stars: abundances

**Abstract** The striking broad emission line spectroscopic appearance of Wolf-Rayet stars have long defied analysis due to the extreme physical conditions of their line and continuum forming regions. Recently, model atmosphere studies have advanced sufficiently to enable the determination of stellar temperatures, luminosities, elemental abundances, ionizing fluxes and wind properties. The observed distribution of nitrogen (WN) and carbon (WC) sequence WR stars in the Milky Way and nearby star forming galaxies is discussed, from which lower limits to progenitor masses are  $\sim 25$ ,  $40$ ,  $75 M_{\odot}$  for hydrogen-depleted (He-burning) WN, WC, and H-rich (H-burning) WN stars, respectively. WR stars in massive binaries permit studies of wind-wind interactions and dust formation in WC systems, plus current mass determinations, revealing typically  $10$ – $25 M_{\odot}$ , although extending up to  $80 M_{\odot}$  for H-rich WN stars. Theoretical and observational evidence in favour of a metallicity dependence of WR winds is presented, with implications for evolutionary models, ionizing fluxes, and the role of WR stars within the context of core-collapse supernovae and long-duration gamma ray bursts.

## CONTENTS

Introduction	3
--------------	---

Observed Properties . . . . .	5
<i>Spectral Properties</i> . . . . .	5
<i>Absolute magnitudes</i> . . . . .	7
<i>Observed distribution</i> . . . . .	8
<i>Binary statistics and masses</i> . . . . .	13
<i>Rotation</i> . . . . .	14
<i>Stellar wind bubbles</i> . . . . .	15
Physical Properties . . . . .	16
<i>Radiative Transfer</i> . . . . .	16
<i>Stellar Temperatures and Radii</i> . . . . .	17
<i>Stellar Luminosities</i> . . . . .	20
<i>Ionizing fluxes</i> . . . . .	21
<i>Elemental abundances</i> . . . . .	23
Wind Properties . . . . .	27
<i>Wind velocities</i> . . . . .	27
<i>Mass-loss rates</i> . . . . .	28
<i>Clumping</i> . . . . .	29
<i>Metallicity dependent winds?</i> . . . . .	31
<i>Line driving in WR winds</i> . . . . .	34
Interacting Binaries . . . . .	38
<i>Close binary evolution</i> . . . . .	38
<i>Colliding winds</i> . . . . .	39
<i>Dust formation</i> . . . . .	41
Evolutionary models and properties at core-collapse . . . . .	43
<i>Rotational mixing</i> . . . . .	43
<i>Evolutionary model predictions</i> . . . . .	45
<i>WR stars as SNe and GRB progenitors</i> . . . . .	47

Summary Points . . . . .	50
Future Issues to be Resolved . . . . .	51

## 1 Introduction

Massive stars dominate the feedback to the local interstellar medium (ISM) in star-forming galaxies via their stellar winds and ultimate death as core-collapse supernovae. In particular, Wolf-Rayet (WR) stars, typically possess wind densities an order of magnitude higher than massive O stars, contribute to the chemical enrichment of galaxies, represent the prime candidates for the immediate progenitors of long, soft Gamma Ray Bursts (GRBs, Woosley & Bloom 2006) and provide a signature of high-mass star formation in galaxies (Schaerer & Vacca 1998).

Three stars in Cygnus with broad emission lines of highly excited elements were first identified by Wolf & Rayet (1867), after whom the class was named. Spectroscopically, WR stars are spectacular in appearance, with strong broad emission lines, instead of narrow absorption lines which are typical of normal stellar populations (e.g. Beals 1940). It was immediately apparent that their spectra came in two flavours, subsequently identified as those with strong lines of helium and nitrogen (WN subtypes) and those with strong helium, carbon, and oxygen (WC and WO subtypes). Gamov (1943) first suggested that the anomalous composition of WR stars was the result of nuclear processed material being visible on their surfaces, although this was not universally established until the final decade of the 20th Century (Lamers et al. 1991). Specifically, WN and WC stars show the products of the CNO cycle (H-burning) and the triple- $\alpha$  (He-burning), respectively. In reality, there is a continuity of physical and chemical properties between O supergiants and WN subtypes.

Typically, WR stars possess masses of  $10\text{--}25 M_{\odot}$ , such that they are descended from O stars with typically  $40 M_{\odot}$ , spending  $\sim 10\%$  of its 5Myr lifetime as a WR star (Meynet & Maeder 2005). The minimum initial mass for a star to become a WR star at Solar metallicity is  $\sim 25 M_{\odot}$ , which corresponds closely to the Humphreys & Davidson (1979) limit for red supergiants (RSG), according to a comparison between the current temperature calibration of RSG and stellar models allowing for mass-loss and rotation (e.g. Levesque et al. 2005). Consequently, within a fairly limited mass range of probably  $25\text{--}30 M_{\odot}$  some single WR objects are post-RSG stars, whilst evolution proceeds via an intermediate Luminous Blue Variable (LBV) phase above  $30 M_{\odot}$ . For close binaries, the critical mass for production of a WR star has no such robust lower limit, since Roche Lobe overflow or common envelope evolution could produce a WR star in preference to an extended RSG phase.

The strong, broad emission lines seen in spectra of WR stars are due to their powerful stellar winds. The wind is sufficiently dense that an optical depth of unity in the continuum arises in the outflowing material. The spectral features are formed even further out and are found primarily in emission. The line and continuum formation regions are geometrically extended compared to the stellar radius and their physical depth in the star highly wavelength dependent. Their unique spectroscopic signature has permitted their detection individually in Local Group galaxies (e.g. Massey & Johnson 1998), collectively within knots of local star forming galaxies (e.g. Hadfield & Crowther 2006), and as significant contributors to the average rest-frame UV spectrum of Lyman Break Galaxies (Shapley et al. 2003).

The present review focuses on observational properties of massive Wolf-Rayet

stars in the Milky Way and beyond, plus physical and chemical properties determined from spectroscopic analysis, plus comparisons with interior evolutionary models. Low mass central stars of Planetary Nebulae displaying a Wolf-Rayet spectroscopic appearance (denoted [WR]) are not considered, although analysis tools discussed here are common to both types of star (e.g. Crowther et al. 2006a).

## 2 Observed Properties

### 2.1 Spectral Properties

Visual spectral classification of WR stars is derived from emission line strengths and line ratios following Smith (1968a). WN spectral subtypes utilize a scheme, involving line ratios of N III-v and He I-II, ranging from WN2 to WN5 for ‘early WN’ (WNE) stars, and WN7 to WN9 for ‘late WN’ (WNL) stars, with WN6 stars either early or late-type. A ‘h’ suffix may be used to indicate the presence of emission lines due to hydrogen (Smith, Shara & Moffat 1996). Complications arise for WN stars with intrinsically weak emission lines, such as WR24 (WN6ha), with a He II 4686 equivalent width an order of magnitude smaller than some other WN6 stars, for which the ‘ha’ nomenclature indicates both intrinsic absorption and emission hydrogen lines. From a standard spectroscopic viewpoint such stars possess mid to late WN spectral classifications. However, their appearance is rather more reminiscent of Of stars than classic WN stars, since there exists a continuity of properties between normal O stars and late-type WN stars. These stars are widely believed to be massive O stars with relatively strong stellar winds at a rather early evolutionary stage, rather than the more mature, classic He-burning WN stars.

Smith, Crowther & Prinja (1994) extended the WN sequence to very late WN10–11 subtypes, in order to include a group of emission line stars originally classified as Ofpe/WN9 (Bohannan & Walborn 1989). WN11 subtypes closely resemble extreme early-type B supergiants, except for the presence of He II  $\lambda 4686$  emission. Indeed, R127 (WN11) in the Large Magellanic Cloud (LMC), was later identified as a LBV (Stahl et al. 1983), whilst a famous Galactic LBV, AG Car exhibited a WN11-type spectrum at visual minimum (Walborn 1990; Smith et al. 1994).

Various multi-dimensional systems have been proposed for WN stars, generally involving line strength or width, such that strong/broad lined stars have been labelled WN-B (Hiltner & Schild 1966), WN-s (Hamann, Koesterke & Wessolowski 1993) or WNb (Smith, Shara & Moffat 1996), none of which have been generally adopted. From a physical perspective, strong and weak lined WN stars do form useful sub-divisions, such that we shall define weak (-w) and strong (-s) WN stars as those with He II 5412 equivalent widths smaller or larger than 40Å. An obvious limitation with such an approach is that intrinsically strong-lined WN stars would be diluted by binary companions or nearby stars in spatially crowded regions, and so would not necessarily qualify as such. WNE-w stars tend to exhibit triangular line profiles rather than the more typical Gaussian lines of WNE-s stars (Marchenko et al. 2004), since one observes material much closer to the stellar core that is being strongly accelerated.

WC spectral subtypes depend on the line ratios of C III and C IV lines along with the appearance of O III-v, spanning WC4 to WC9 subtypes, for which WC4–6 stars are ‘early’ (WCE) and WC7–9 are ‘late’ (WCL). Rare, oxygen-rich WO stars form an extension of the WCE sequence, exhibiting strong O VI  $\lambda\lambda 3811$ –34

emission (Kingsburgh, Barlow & Storey 1995). The most recent scheme involves WO1 to WO4 subtypes depending on the relative strength of O v-vi and C IV emission lines (Crowther, De Marco & Barlow 1998). Finally, C IV  $\lambda$ 5801-12 appears unusually strong in an otherwise normal WN star in a few cases, leading to an intermediate WN/C classification (Conti & Massey 1989). WN/C stars are indeed considered to be at an intermediate evolutionary phase between the WN and WC stages.

Representative examples of WN and WC stars are presented in Figure 1. Various X-ray to mid-IR spectroscopic datasets of Galactic Wolf-Rayet stars are presented in Table 1, including extreme ultraviolet synthetic spectra from model atmospheres (Smith, Norris & Crowther 2002; Hamann & Gräfener 2004).

## 2.2 Absolute magnitudes

Standard optical UBV photometry does not permit WR stars to be distinguished from normal hot stars. Broad-band visual measurements may overestimate the true continuum level in extreme cases by up to 1 magnitude, or more typically 0.5 mag for single early-type WR stars due to their strong emission line spectra. Consequently, narrow band *uby*<sub>r</sub> filters were introduced by Westerlund (1966), specifically designed to minimize the effect of WR emission lines (but their effect cannot be entirely eliminated). These were later refined by Smith (1968b) and Massey (1984), such that most photometry of WR stars has used the *ubvr* filter system, which is compared to Johnson UBV filters in Fig. 1.

As with normal stars, *ubv* photometry permits a determination of the interstellar extinction,  $A_v$ . If we adopt  $R = A_V/E(B - V) = 3.1$ , the broad and

narrow-band optical indices for WR stars are related by

$$A_v = 4.12 E_{b-v} = 3.40 E_{B-V} = 1.11 A_V$$

following Turner (1982). Due to their large distances, direct determination via stellar parallax methods are only possible for the sole case of  $\gamma$  Vel (WC8+O) using *Hipparcos*, and even that remains controversial. Otherwise, cluster or association membership is used to provide an approximate absolute magnitude-spectral type calibration for Milky Way WR stars. The situation is much better for WR stars in the Magellanic Clouds, although not all subtypes are represented. Typical absolute magnitudes range from  $M_v = -3$  mag at earlier subtypes to  $-6$  mag for late subtypes, or exceptionally  $-7$  mag for hydrogen rich WN stars, with a typical spread of  $\pm 0.5$  mag at an individual subtype.

### 2.3 Observed distribution

Conti (1976) first proposed that a massive O star may lose a significant amount of mass via stellar winds, revealing first the H-burning products at its surface, and subsequently the He-burning products, which have been spectroscopically identified with the WN and WC phases. Such stars should be over-luminous for their mass, in accord with observations of WR stars in binary systems. This general sequence has since become known as the ‘Conti scenario’. Massey (2003) provides a more general overview of massive stars within Local Group galaxies.

2.3.1 WR STARS IN MILKY WAY Wolf-Rayet stars are located in or close to massive star forming regions within the Galactic disk, for which a catalogue is provided by van der Hucht (2001). A quarter of the known WR content of the Milky Way reside within massive clusters at the Galactic Centre or in Westerlund 1 (van der Hucht 2006). From membership of WR stars in open clusters, Schild &

Maeder (1984) and Massey, DeGioia-Eastwood & Waterhouse (2001) investigated the initial masses of WR stars empirically, for which a revised compilation is provided in Crowther et al. (2006b). Overall, hydrogen-rich WN stars (WNha) are observed in young massive clusters, from which main sequence turn-off masses (based on Meynet et al. 1994 isochrones) suggest initial masses in excess of  $\geq 65 - 110M_{\odot}$ , and are believed to be core-H burning (Langer et al. 1994; Crowther et al. 1995a). Lower mass progenitors of initial masses  $40-50M_{\odot}$  are suggested for classic mid-WN, late WC and WO stars. Progenitors of some early WN stars appear to be less massive still, suggesting an initial mass cutoff for WR stars at Solar metallicity around  $25M_{\odot}$ .

From an evolutionary perspective, the absence of RSGs at high luminosity and presence of H-rich WN stars in young massive clusters suggests the following variation of the Conti scenario in the Milky Way, i.e. for stars initially more massive than  $\sim 75M_{\odot}$

$$O \rightarrow \text{WN(H-rich)} \rightarrow \text{LBV} \rightarrow \text{WN(H-poor)} \rightarrow \text{WC} \rightarrow \text{SNIc}$$

whilst for stars of initial mass from  $\sim 40 - 75M_{\odot}$ ,

$$O \rightarrow \text{LBV} \rightarrow \text{WN(H-poor)} \rightarrow \text{WC} \rightarrow \text{SNIc}$$

and for stars of initial mass in the range  $25-40M_{\odot}$

$$O \rightarrow \text{LBV/RSG} \rightarrow \text{WN(H-poor)} \rightarrow \text{SNIb.}$$

Indeed, the role of the LBV phase is not yet settled – either this stage may be circumvented entirely in some cases, follow the RSG stage, or even alternatively dominate pre-WR mass-loss for the most massive stars (Langer et al. 1994; Smith & Owocki 2006). Conversely, the presence of dense, circumstellar shells around

Type IIn SN indicates that some massive stars may even undergo core-collapse during the LBV phase (Gal-Yam et al. 2006). Remarkably few Milky Way clusters host both RSG and WR stars, with the notable exception of Westerlund 1 (Clark et al. 2005), suggesting a fairly narrow mass range common to both populations.

Although optical narrow-band surveys (see below) have proved very successful for identifying WR stars in the Solar neighbourhood, only a few hundred WR stars are known in the Milky Way, whilst many thousands are expected within the Galactic disk (van der Hucht 2001). Consequently, near-IR narrow-band imaging surveys together with spectroscopic follow-up may be considered for more extensive surveys to circumvent high interstellar extinction (Homeier et al. 2003). Limitations of IR emission line surveys are that near-IR line fluxes are much weaker than optical lines, plus no strong WR lines are common to all spectral types in the frequently used K-band. An added complication is that dust forming WC stars heavily dilute emission lines longward of the visual. Nevertheless, such surveys are presently underway towards an improved census of WR stars in the Milky Way. Alternatively, WR candidates may be identified from their near to mid-IR colours, which, along with other high wind density supergiants, are unusually flat due to strong free-free excess emission (Hadfield et al. 2007).

**2.3.2 WR STARS IN LOCAL GROUP** WR stars have typically been discovered via techniques sensitive to their unusually broad emission line spectra, based on objective prism searches or interference filter imaging. Narrow-band interference filter techniques have been developed (e.g. Moffat, Seggewiss & Shara 1985; Massey, Armandroff & Conti 1986) that distinguished strong WR emission lines at He II  $\lambda 4686$  (WN stars) and C III  $\lambda 4650$  (WC stars) from the nearby con-

tinuum. Such techniques have been applied to regions of the Milky Way disk, Magellanic Clouds and other nearby galaxies. An example of this approach is presented in Figure 2 for the spiral galaxy NGC 300 ( $d \sim 2$  Mpc). A wide-field image of NGC 300 is presented, with OB complex IV-V indicated, together with narrow-band images centred at  $\lambda 4684$  (He II 4686) and  $\lambda 4781$  (continuum). Several WR stars are indicated in the difference (He II-continuum) image, including an apparently single WC4 star (Schild et al. 2003).

It is well established that the absolute number of WR stars, and their subtype distribution is metallicity dependent.  $N(\text{WR})/N(\text{O}) \sim 0.15$  in the relatively metal-rich Solar Neighbourhood (Conti et al. 1983; van der Hucht 2001), whilst  $N(\text{WR})/N(\text{O}) \sim 0.01$  in the metal-deficient SMC on the basis of only 12 WR stars (Massey, Olsen & Parker 2003) versus  $\sim 1000$  O stars (Evans et al. 2004). It is believed that the majority of Galactic WR stars are the result of single star evolution, whilst some stars (e.g. V444 Cyg) result from close binary evolution (Vanbeveren et al. 1998). One might suspect that most WR stars in metal-poor environments are formed via binary evolution, yet Foellmi, Moffat & Guerrero (2003a) suggest a similar WR binary fraction for the SMC and Milky Way.

Similar numbers of WN to WC stars are known in the Solar Neighbourhood (van der Hucht 2001, 2006), whilst WN stars exceed WC stars by a factor of  $\sim 5$  and  $\sim 10$  for the LMC and SMC, respectively (Breysacher, Azzopardi & Testor 1999; Massey, Olsen & Parker 2001). At low metallicity the reduced WR population, and relative dominance of WN subtypes, most likely results from the metallicity dependence of winds from their evolutionary precursors (Mokiem et al. 2007), such that only the most massive single stars reach the WR phase. Single stars that reach the WC phase at high metallicity, may end their life as a

RSG or a WN star in a lower metallicity environment.

Not all WR subtypes are observed in all environments. Early WN and WC subtypes are preferred in low metallicity galaxies, while the reverse is true at high metallicity. Line widths of early WC and WO stars are higher than late WC stars, although width alone is not a defining criterion for each spectral type. The correlation between WC subclass and line width is nevertheless strong (Torres, Conti & Massey 1986). The subtype distribution of WR stars in the Solar Neighbourhood, LMC and SMC is presented in Figure 3. We shall address this aspect in Sect 4.4.

**2.3.3 WR GALAXIES** Individual WR stars may, in general, be resolved in Local Group galaxies from ground-based observations, whilst the likelihood of contamination by nearby sources increases at larger distance. For example, a typical slit width of  $1''$  at the 2 Mpc distance of NGC 300 corresponds to a spatial scale of  $\sim 10$  pc. Relatively isolated WR stars have been identified, albeit in the minority (recall Figure 2). This is even more problematic for more distant galaxies, such as M 83 where the great majority of WR stars are observed in clusters or associations (Hadfield et al. 2005). So-called ‘WR galaxies’ are typically starburst regions exhibiting spectral features from tens, hundreds or even thousands of WR stars (Schaerer, Contini & Pindao 1999).

Average Milky Way/LMC WN or WC line fluxes (Schaerer & Vacca 1998) are typically used to calculate stellar populations in WR galaxies. These should be valid providing the line fluxes of WR templates do not vary with environment. However, it is well known that SMC WN stars possess weak emission lines (Conti, Garmany & Massey 1989). In spite of small statistics and a large scatter, the mean He II  $\lambda 4686$  line luminosity of WN2–4 stars in the LMC is  $10^{35.9}$  erg s $^{-1}$ , a

factor of five times higher than the mean of equivalent stars in the SMC (Crowther & Hadfield 2006). Providing extinction is low, the signature of WN stars is most readily seen at ultraviolet wavelengths, where the dilution from other stellar types is at its weakest (e.g. Hadfield & Crowther 2006). The strongest UV, optical and near-IR lines indicate flux ratios of  $I(\text{He II } 1640)/I(\text{He II } 4686) \sim 10$  and  $I(\text{He II } 4686)/I(\text{He II } 1.012\mu\text{m}) \sim 6$  for WN stars spanning SMC to Milky Way metallicities.

Similar comparisons for WC stars are hindered because the only carbon sequence WR stars at the low metallicity of the SMC and IC 1613 are WO stars, which are systematically weaker than WC stars in the LMC and Milky Way (Kingsburgh et al. 1995; Kingsburgh & Barlow 1995; Schaerer & Vacca 1998). The mean C IV  $\lambda\lambda 5801-2$  line luminosity of WC4 stars in the LMC is  $10^{36.5} \text{ erg s}^{-1}$  (Crowther & Hadfield 2006). Again, detection of WC stars is favoured via ultraviolet spectroscopy, owing to line flux ratios of  $I(\text{C IV } 1548-51)/I(\text{C IV } 5801-12) \sim 6$  and  $I(\text{C IV } 5801-12)/I(\text{C IV } 2.08\mu\text{m}) \sim 15$ .

## 2.4 Binary statistics and masses

The observed binary fraction amongst Milky Way WR stars is 40% (van der Hucht 2001), either from spectroscopic or indirect techniques. Within the low metallicity Magellanic Clouds, close binary evolution would be anticipated to play a greater role because of the diminished role of O star mass-loss in producing single WR stars. However, where detailed studies have been carried out (Bartzakos, Moffat & Niemela 2001; Foellmi, Moffat & Guerrero 2003ab), a similar binary fraction to the Milky Way has been obtained (recall Figure 3), so metallicity-independent LBV eruptions may play a dominant role.

The most robust method of measuring stellar masses is from Kepler's third law of motion, particularly for eclipsing double-lined (SB2) systems, from which the inclination may be derived. Orbital inclinations may also be derived from linear polarization studies (e.g. St-Louis et al. 1993) or atmospheric eclipses (Lamontagne et al. 1996). Masses for Galactic WR stars are included in the van der Hucht (2001) compilation, a subset of which are presented in Figure 4 together with some more recent results. WC masses span a narrow range of 9– $16M_{\odot}$ , whilst WN stars span a very wide range of  $\sim 10$ – $83M_{\odot}$ , and in some cases exceed their OB companion, i.e.  $q = M_{\text{WR}}/M_O > 1$  (e.g. WR22: Schweickhardt et al. 1999). WR20a (SMSp2) currently sets the record for the highest orbital-derived mass of any star, with  $\sim 83M_{\odot}$  for each WN6ha component (Rauw et al. 2005). As discussed above, such stars are H-rich, extreme O stars with strong winds rather than classical H-poor WN stars, albeit a factor of two lower than the apparent  $\sim 150M_{\odot}$  stellar mass limit (Figer 2005), such that still more extreme cases may yet await discovery. Spectroscopic measurement of masses via surface gravities using photospheric lines is not possible for WR stars due to their dense stellar winds.

## 2.5 Rotation

Observationally, rotation is very difficult to measure in WR stars, since photospheric features – used to estimate  $v \sin i$  in normal stars – are absent. High rotational velocities of 200–500 km s $^{-1}$  have been reported for WR138 (Massey 1980) and WR3 (Massey & Conti 1981), although the former has a late-O binary companion, and the absorption lines of the latter are formed within the stellar wind (Marchenko et al. 2004). Fortunately, certain WR stars harbour large scale

structures, from which an inferred rotation period may be inferred (St-Louis et al. 2006). Alternatively, if WR stars were rapid rotators, one would expect strong deviations from spherical symmetry due to gravity darkening (Von Zeipel 1924; Owocki, Cranmer & Gayley 1996).

Harries, Hillier & Howarth (1998) studied linear spectropolarimetric datasets for 29 Galactic WR stars, from which just four single WN stars plus one WC+O binary revealed a strong line effect, suggesting significant departures from spherical symmetry. They presented radiative transfer calculations which suggest that the observed continuum polarizations for these stars can be matched by models with equator to pole density ratios of 2–3. Of course, the majority of Milky Way WR stars do not show a strong linear polarization line effect (e.g. Kurosawa, Hillier & Schulte-Ladbeck (1999)).

## 2.6 Stellar wind bubbles

Ring, or ejecta nebulae, composed of material ejected during the RSG or LBV phases – but photo-ionized by the WR star – are observed for a subset of WR stars. The first known examples, NGC 2359 and NGC 6888, display a shell morphology, although many subsequently detected in the Milky Way and Magellanic Clouds exhibit a variety of spatial morphologies (Chu, Treffers & Kwitter 1983; Dopita et al. 1994). Nebulae are predominantly associated with young WR stars i.e. primarily WN subtypes, with typical electron densities of  $10^2$  cm $^{-3}$  to  $10^3$  cm $^{-3}$  (Esteban et al. 1993).

Ring nebulae provide information on evolutionary links between WR stars and their precursors (Weaver et al. 1977). Once a massive star has reached the WR phase, its fast wind will sweep up the material ejected during the immediate pre-

cursor (LBV or RSG) slow wind. The dynamical evolution of gas around WR stars with such progenitors is discussed by García-Segura, MacLow & Langer (1996a) and García-Segura, Langer & MacLow (1996b), respectively. Esteban et al. (1993) attempted to derive WR properties indirectly from H II regions associated with selected Milky Way stars (see also Crowther et al. 1999). Unfortunately, relatively few H II regions are associated with individual WR stars, and for the majority of these, the nebular parameters are insufficiently well constrained to distinguish between different stellar atmosphere models.

### 3 Physical Properties

#### 3.1 Radiative Transfer

Our interpretation of hot, luminous stars via radiative transfer codes is hindered with respect to normal stars by several effects. First, the routine assumption of LTE breaks down for high temperature stars. In non-LTE, the determination of populations uses rates which are functions of the radiation field, itself a function of the populations. Consequently, it is necessary to solve for the radiation field and populations, requiring an iterative approach.

Secondly, the problem of accounting for the effect of millions of spectral lines upon the emergent atmospheric structure and emergent spectrum – known as line blanketing – remains challenging for stars in which spherical, rather than plane-parallel, geometry is necessary due to stellar winds, since the scale height of their atmospheres is no longer negligible with respect to their stellar radii. The combination of non-LTE, line blanketing (and availability of atomic data thereof), and spherical geometry has prevented the routine analysis of such stars until recently.

Radiative transfer is either solved in the co-moving frame, as applied by CMF-GEN (Hillier & Miller 1998) and PoWR (Gräfener, Koesterke & Hamann 2002) or via the Sobolev approximation, as used by ISA-wind (de Koter, Schmutz & Lamers 1993). The incorporation of line blanketing necessitates one of several approximations. Either a ‘super-level’ approach is followed, in which spectral lines of a given ion are grouped together in the solution of the rate equations (Anderson 1989), or alternatively, a Monte Carlo approach is followed, which uses approximate level populations (Abbott & Lucy 1985).

### 3.2 Stellar Temperatures and Radii

Stellar temperatures for WR stars are difficult to characterize, since their geometric extension is comparable with their stellar radii. Atmospheric models for WR stars are typically parameterized by the radius of the inner boundary,  $R_*$ , at large optical depth, typically  $\tau_{\text{Ross}} \sim 10$ . However, only the optically thin part of the atmosphere is seen by the observer, such that  $R_*$  relies upon the same velocity law holding for the invisible, optically thick part. The optical continuum radiation originates from a ‘photosphere’ where the Rosseland optical depth reaches 2/3. Typical WN and WC winds have reached a significant fraction of their terminal velocity before they become optically thin in the continuum, such that the radius at an optical depth of 2/3,  $R_{2/3}$ , lies at supersonic velocities, well beyond the hydrostatic domain. For example, Crowther et al. (2006a) obtain  $R_* = 2.9 R_\odot$  and  $R_{2/3} = 7.7 R_\odot$  for HD 50896 (WN4b), corresponding to  $T_* = 85\text{kK}$  and  $T_{2/3} = 52\text{kK}$ , respectively. In some weak-lined early-type WN stars, this is not strictly true since their spherical extinction is modest, such that  $R_* \sim R_{2/3}$  (e.g. WR3: Marchenko et al. 2004).

Figure 5 compares  $R_*$ ,  $R_{2/3}$  and the principal optical (wind) line forming region ( $\log n_e = 10^{11}$  to  $10^{12}$  cm $^{-3}$ ) for HD 66811 ( $\zeta$  Pup, O4I(n)f), HD 96548 (WR40, WN8) and HD 164270 (WR103, WC9) on the same physical scale. Some high ionization spectral lines (e.g. N V and C IV lines in the WN8 and WC9 star respectively) are formed at higher densities of  $n_e \geq 10^{12}$  cm $^{-3}$  in the WR winds. Their high wind densities require the simultaneous determination of mass-loss rate and stellar temperature from non-LTE model atmosphere fits to observations, since their atmospheres are so highly stratified.

Stellar temperatures of WR stars are determined using emission lines from ions of nitrogen or helium (WN stars), or carbon (WC stars). Initial non-LTE models for WR stars consisted solely of helium (Hillier 1987). Subsequently, hydrogen (Hamann et al. 1991) and CNO elements (Hillier 1988) were included – still neglecting Fe-peak elements – with a modest increase upon the derived temperatures of WN stars, but a dramatic effect on WC stars, for which large carbon (and oxygen) abundances have a dominant effect upon the wind structure, leading to much higher WC temperatures. Metals such as C, N and O provide efficient coolants, as in H II regions, such that the outer wind electron temperature is typically 8,000K to 12,000K in WR atmospheres, in dramatic contrast to very high stellar temperatures (Hillier 1988, 1989).

Once line blanketing by iron group elements is included, stellar temperatures and more importantly bolometric corrections and stellar luminosities increase, by significant factors in most cases (Schmutz 1997; Hillier & Miller 1999). Until recently, the number of stars studied with non-LTE, clumped, line blanketed models has been embarrassingly small, due to the need for detailed, tailored analysis of individual stars using a large number of free parameters. Recently,

Hamann, Gräfener & Liermann (2006) have applied their grid of line blanketed WR models to the analysis of most Galactic WN stars, for the most part resolving previous discrepancies between alternate line diagnostics, identified by Crowther et al. (1995b). To date, only a limited number of WC stars in the Milky Way and Magellanic Clouds have been studied in detail (e.g. Dessart et al. 2000; Crowther et al. 2002; Barniske, Hamann & Gräfener 2006).

Stellar temperatures of WR stars, relating to  $R_*$ , range from 30kK amongst WN10 subtypes to 40kK at WN8 and approach 100kK for early-type WN stars. Spectroscopic temperatures are rather higher on average for WC stars, i.e. 50kK for WC9 stars, increasing to 70kK at WC8 and  $\sim$ 100kK for early WC. Spectroscopically derived temperatures of Galactic WR subtypes are presented in Table 2, where we have separated strong and weak-lined WN3–6 which differ in wind densities, and include parameters for representative LMC WC4 and WO stars.

Stellar structure models predict radii which are significantly smaller than those derived from atmospheric models, i.e.  $R_* = 2.7R_\odot$  for HD 191765 (WR134, WN6b) in Table 2, versus  $R_{\text{evol}} = 0.8R_\odot$  which follows from hydrostatic evolutionary models, namely

$$\log \frac{R_{\text{evol}}}{R_\odot} = -1.845 + 0.338 \log \frac{L}{L_\odot} \quad (1)$$

for hydrogen-free WR stars (Schaerer & Maeder 1992). Theoretical corrections to such radii are frequently applied, although these are based upon fairly arbitrary assumptions, which relate particularly to the velocity law. Consequently, a direct comparison between temperatures of most WR stars from evolutionary calculations and empirical atmospheric models is not straightforward, except that one requires  $R_{2/3} > R_{\text{evol}}$ , with the difference attributed to the extension of the su-

personice region. Petrovic, Pols & Langer (2006) established that the hydrostatic cores of metal-rich WR stars above  $\sim 15M_{\odot}$  exceed Eqn 1 by significant factors if mass-loss is neglected, due to their proximity to the Eddington limit,  $\Gamma_e = 1$ . Here, the Eddington parameter,  $\Gamma_e$ , is the ratio of radiative acceleration due to Thompson (electron) scattering to surface gravity and may be written as

$$\Gamma_e = 10^{-4.5} q \frac{L/L_{\odot}}{M/M_{\odot}} \quad (2)$$

where the number of free electrons per atomic mass unit is  $q$ . In reality, high empirical WR mass-loss rates imply that inflated radii are not expected, such that the discrepancy in hydrostatic radii between stellar structure and atmospheric models has not yet been resolved.

### 3.3 Stellar Luminosities

Individual bolometric corrections range from  $-2.7$  mag amongst very late WN stars (Crowther & Smith 1997) to approximately  $-6$  mag for weak-lined, early-type WN stars and WO stars (Crowther et al. 1995b; Crowther et al. 2000). For absolute magnitudes of WR stars – obtained from cluster or association membership (van der Hucht 2001) – luminosities of He-burning WR stars in the Milky Way range from  $\sim 100,000 L_{\odot}$  for WC stars to  $200,000 L_{\odot}$  for early WN stars, and a factor of 2 times higher for late WN stars containing hydrogen, as shown in Table 2, from which it can be seen that LMC WC stars are several times more luminous than Milky Way WC counterparts. Late-type WNha stars, which are thought to be H-burning O stars with strong winds, have luminosities in excess of  $10^6 L_{\odot}$ .

From stellar structure theory, there is a mass-luminosity relation for H-free

WR stars which is described by

$$\log \frac{L}{L_\odot} = 3.032 + 2.695 \log \frac{M}{M_\odot} - 0.461 \left( \log \frac{M}{M_\odot} \right)^2. \quad (3)$$

This expression is effectively independent of the chemical composition since the continuum opacity is purely electron scattering (Schaerer & Maeder 1992). Spectroscopic luminosities need to be corrected for that powering the stellar wind,  $\frac{1}{2} \dot{M} v_\infty^2$ , in order to determine the underlying nuclear luminosity,  $L_{\text{nuc}}$ . In most cases, the recent reduction in mass-loss rates due to wind clumping (see Sect. 4.3), and increase in luminosities due to line blanketing, indicate a fairly modest corrective factor. From Table 2, one expects typical masses of  $10\text{--}15M_\odot$  for hydrogen-free WR stars, which agree fairly well with binary mass estimates (recall Fig. 4). Indeed, it is possible to compare spectroscopically derived WR masses obtained using this relationship with binary masses in a few cases (e.g.  $\gamma$  Vel: De Marco et al. 2000).

Systematically higher spectroscopic luminosities have been recently determined by Hamann, Gräfener & Liermann (2006) for Galactic WN stars, since they adopt uniformly high  $M_v = -7.2$  mag for all non-cluster WN6–9h stars. Absolute magnitudes for normal late WN stars are subject to large uncertainties since they positively shy away from clusters. As a consequence, their results suggest a bi-modal distribution around  $300,000 L_\odot$  for early WN stars, and  $1\text{--}2 \times 10^6 L_\odot$  for all late WN stars.

### 3.4 Ionizing fluxes

The Lyman continuum ionizing flux distributions of WR stars in general extend those for O stars to higher temperature, and so significant HeI continua are obtained, with strong HeII continua in a few high temperature, low density cases.

Lyman continuum ionizing fluxes,  $N(\text{LyC})$ , are typical of mid-O stars in general (Table 2), such that WR stars are expected to play only a minor role in the ionizing budget due to the low ratio of  $N(\text{WR})/N(\text{O})$  in star forming regions, with the exception of the H-rich WN stars which compare closely to O2 stars (Walborn et al. 2004). Indeed, Crowther & Dessart (1998) showed that the WN6ha stars in NGC 3603 provided  $\sim 20\%$  of the Lyman continuum ionizing photons, based upon calibrations of non-blanketed models for O and WR stars.

The primary effect of blanketing is to re-distribute extreme UV flux to longer wavelengths, reducing the ionization balance in the wind, such that higher temperatures and luminosities are required to match the observed WR emission line profile diagnostics relative to unblanketed studies. Recent revisions to temperatures and luminosities of O stars (as measured from photospheric lines) have acted in the reverse sense, relative to previous plane-parallel unblanketed model analysis, due to backwarming effects, as shown in a number of recent papers (e.g. Martins, Schaerer & Hillier 2002; Repolust, Puls & Herrero 2004). Common techniques are generally now employed for O and WR studies, such that a factor of two increase in  $N(\text{LyC})$  for WR stars – with the reverse for O stars – suggests that in such cases WR stars might provide close to half of the total ionizing photons in the youngest starbursts.

The strength of WR winds impacts upon the hardness of their ionizing radiation. Atmospheric models for high wind density WR stars produce relatively soft ionizing flux distributions, in which extreme UV photons are redistributed to longer wavelength by the opaque stellar wind (Schmutz, Leitherer & Gruenwald 1992). In contrast, for the low wind density case, a hard ionizing flux distribution is predicted, in which extreme UV photons pass through the relatively transpar-

ent wind unimpeded. Consequently, the shape of the ionizing flux distribution of WR stars is dependent on both the wind density and the stellar temperature. We shall show in Section 4 that low metallicity WR stars possess weaker winds. In Figure 6, we compare the predicted Lyman continuum ionizing flux distribution from four 100kK WN models, in which only the low metallicity, low mass-loss rate models predicts prodigious photons below the  $\text{He}^+$  edge at 228Å.

One expects evidence of hard ionizing radiation from WR stars (e.g. nebular  $\text{He II}$  4686) solely at low metallicities, which is generally borne out by observations of H II regions associated with WR stars (Garnett et al. 1991). Previous studies of metal-rich regions have claimed a low limit to the stellar mass function from indirect H II region studies at high metallicity, in which WR stars were spectroscopically detected. Gonzalez Delgado et al. (2002) were able to reconcile a high stellar mass limit from UV spectral synthesis techniques with a soft ionizing spectrum for the metal-rich WR galaxy NGC 3049 by applying the Smith, Norris & Crowther (2002) line blanketed grid of WR models at high metallicity.

### 3.5 Elemental abundances

For WR stars, it has long been suspected that abundances represented the products of core nucleosynthesis, although it has taken the development of non-LTE model atmospheres for these to have been empirically supported.

**3.5.1 WN AND WN/C STARS** Balmer-Pickering decrement studies by Conti, Leep & Perry (1983) concluded that hydrogen was severely depleted in WR stars. A clear subtype effect regarding the hydrogen content of Galactic WN stars is observed, with late-type WN stars generally showing some hydrogen (typically  $X_H \sim 15 \pm 10\%$ ), and early-type WN stars hydrogen-free, although exceptions do

exist. This trend breaks down within the lower metallicity environment of the Magellanic Clouds, notably the SMC (Foellmi et al 2003a). Milky Way late-type WN stars with weak emission lines – denoted as ‘ha’ due to intrinsic absorption lines plus the presence of hydrogen – are universally H-rich with  $X_H \sim 50\%$  (Crowther et al. 1995a; Crowther & Dessart 1998).

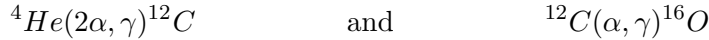
Non-LTE analyses confirm that WN abundance patterns are consistent with material processed by the CNO cycle, in which these elements are used as catalysts, i.e.



in which  $X_N \sim 1\%$  by mass is observed in Milky Way WN stars. Carbon is highly depleted, with typically  $X_C \sim 0.05\%$ . Oxygen suffers from fewer readily accessible line diagnostics, but probably exhibits a similarly low mass fraction as carbon (e.g. Crowther, Smith & Hillier 1995b; Herald, Hillier & Schulte-Ladbeck 2001). Non-LTE analysis of transition WN/C stars reveals elemental abundances (e.g.  $X_C \sim 5\%$ ,  $X_N \sim 1\%$  by mass) which are in good agreement with these stars occupying a brief transition stage between the WN and WC stages (Crowther, Smith & Willis 1995c).

**3.5.2 WC AND WO STARS** Neither hydrogen nor nitrogen is detected in the spectra of WC stars. Recombination line studies, using theoretical coefficients for different transitions are most readily applicable to WC stars, since they show a large number of lines in their optical spectra. Atomic data are most reliable for hydrogenic ions, such as C IV and O VI, so early-type WC and WO stars can be most readily studied. Smith & Hummer (1988) suggested a trend of increasing C/He from late to early WC stars, with C/He=0.04–0.7 by number ( $10\% \leq X_C \leq$

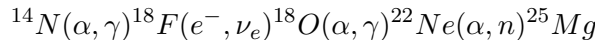
60%), revealing the products of core He burning



although significant uncertainties remain in the latter nuclear reaction rate. These reactions compete during helium burning to determine the ratio of carbon to oxygen at the onset of carbon burning.

In reality, optical depth effects come into play, so detailed abundance determinations for all subtypes can only be carried out using non-LTE model atmospheres. Koesterke & Hamann (1995) indicated refined values of C/He=0.1–0.5 by number ( $20\% \leq X_C \leq 55\%$ ), with no WC subtype dependence, such that spectral types are not dictated by carbon abundance, contrary to suggestions by Smith & Maeder (1991). Indeed, LMC WC4 stars possess similar surface abundances to Milky Way WC stars (Crowther et al. 2002), for which the He II 5412 and C IV 5471 optical lines represent the primary diagnostics (Hillier 1989). These recombination lines are formed at high densities of  $10^{11}$  to  $10^{12}$  cm $^{-3}$  at radii of 3–30  $R_*$  (recall Figure 5). Oxygen diagnostics in WC stars lie in the near-UV, such that derived oxygen abundances are rather unreliable, unless space-based spectroscopy is available. Where they have been derived, one finds  $X_O \sim 5\text{--}10\%$  for WC stars (e.g. Crowther et al. 2002).

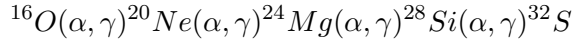
Core He burning in massive stars also has the effect of transforming  $^{14}\text{N}$  (produced in the CNO cycle) to neon and magnesium via



and serves as the main neutron source for the s-process in massive stars. Neon lines are extremely weak in the UV/optical spectrum of WC stars (Crowther et al. 2002), but ground-state fine-structure lines at [Ne II] 12.8 $\mu\text{m}$  and [Ne III]

$15.5\mu\text{m}$  may be observed via mid-IR spectroscopy, as illustrated for  $\gamma$  Vel in van der Hucht et al. (1996). These stellar wind lines, with critical densities of  $10^5\text{ cm}^{-3}$ , are formed at hundreds of stellar radii and may be used to derive neon abundances in WC stars. Barlow, Roche & Aitken (1988) came to the conclusion that neon was not greatly enhanced in  $\gamma$  Vel, for which the Solar abundance is  $\sim 0.1\%$  (primarily  $^{20}\text{Ne}$ ). This was a surprising result since the above reaction is expected to produce  $\sim 2\%$  by mass of  $^{22}\text{Ne}$  at Solar metallicity. It was only when the clumped nature of WR winds was taken into consideration, that neon was found to be enhanced in  $\gamma$  Vel and other WC stars (e.g. Dessart et al. 2000), albeit with only  $\sim 1\%$  by mass (see also Crowther, Morris & Smith 2006a). Meynet & Maeder (2003) note that the  $^{22}\text{Ne}$  enrichment depends upon nuclear reaction rates rather than stellar models, so the remaining disagreement may suggest a problem with the relevant reaction rates, or more likely the reduced Solar oxygen abundance (Asplund et al. 2004).

WO stars are extremely C and O-rich, as deduced from recombination analyses (Kingsburgh, Barlow & Storey 1995), and supported by non-LTE models (Crowther et al. 2000). Further nucleosynthesis reactions produce alpha elements via



producing a core which is initially dominated by  $^{16}\text{O}$  and  $^{20}\text{Ne}$ . *Spitzer* studies are in progress to determine neon abundances in WO stars, in order to assess whether these stars show evidence of  $\alpha$ -capture of oxygen (in which case enhanced  $^{20}\text{Ne}$  would again dominate over  $^{22}\text{Ne}$ ).

## 4 Wind Properties

The existence of winds in early-type stars has been established since the 1960's, when the first rocket UV observations (e.g. Morton 1967) revealed the characteristic P Cygni signatures of mass-loss. Electron (Thompson) scattering dominates the continuum opacity in O and WR stars, whilst the basic mechanism by which their winds are driven is the transfer of photon momentum to the stellar atmosphere through the absorption by spectral lines. The combination of a plethora of line opacity within the same spectral region as the photospheric radiation allows for efficient driving of winds by radiation pressure (Milne 1926). Wind velocities can be directly measured, whilst the determination of wind densities rely on varying complexity of theoretical interpretation. A theoretical framework for mass-loss in normal hot, luminous stars was developed by Castor, Abbott & Klein (1975), known as CAK theory, via line-driven radiation pressure which we shall review.

### 4.1 Wind velocities

The wavelength of the blue edge of saturated P Cygni absorption profiles provides a measure of the asymptotic wind velocity, for which accurate wind velocities of WR stars can be readily obtained (Prinja, Barlow & Howarth 1990; Willis et al. 2004). Alternatively, optical and near-IR He I P Cygni profiles, or mid-IR fine-structure metal lines may be used to derive reliable wind velocities (Howarth & Schmutz 1992; Eenens & Williams 1994; Dessart et al. 2000).

In principle, optical recombination lines of He II and C III-IV may also be used to estimate wind velocities, since these are formed close to the asymptotic flow velocity, although velocities obtained from spectral line modelling is preferable. For

WR stars exhibiting weak winds, whose lines are formed interior to the asymptotic flow velocity, only lower limits may be obtained. Nevertheless, observational evidence suggests lower wind velocities at later subtypes, by up to a factor of ten than early subtypes (Table 2). Wind velocities of LMC WN stars compare closely with Milky Way counterparts. Unfortunately, UV spectroscopy of SMC WN stars is scarce, such that one has to rely on optical emission lines for wind velocity estimates, which provide only lower limits to terminal wind velocities.

The current record holder amongst non-degenerate stars for the fastest stellar wind is the Galactic WO star WR93b for which a wind velocity of  $6000 \text{ km s}^{-1}$  has been obtained from optical recombination lines (Drew et al. 2004). Indeed, individual WO stars have now been identified in a number of external galaxies, such that one observes a reduction in line width (and so wind velocity) for stars of progressively lower metallicity, by a factor of up to two between the Milky Way and IC 1613 (Crowther & Hadfield 2006). Although numbers are small, this downward trend in wind velocity with decreasing metallicity is believed to occur for other O and WR spectral types (e.g. Kudritzki & Puls 2000; Crowther 2000).

## 4.2 Mass-loss rates

The mass-loss rate relates to the velocity field,  $v(r)$  and density,  $\rho(r)$  via the equation of continuity

$$\dot{M} = 4\pi r^2 \rho(r) v(r) \quad (4)$$

for a spherical, stationary wind. WR winds may be observed at IR-mm-radio wavelengths via the free-free (Bremsstrahlung) continuum excess caused by the stellar wind or via UV, optical or near-IR emission lines.

Radio continuum derived mass-loss rates (e.g. Leitherer, Chapman & Koribal-

ski 1997) follow from relatively simple analytical relations - under the assumption of homogeneity and spherical symmetry. The emergent radio flux,  $S_\nu$ , is set by the distance to the star  $d$ , mass-loss rate and terminal velocity as follows

$$S_\nu \propto \left( \frac{\dot{M}}{v_\infty} \right)^{4/3} \frac{\nu^\alpha}{d^2} \quad (5)$$

(Wright & Barlow 1975), where  $\alpha \sim 0.6$  in the constant velocity regime. Accurate determinations of WR mass-loss rates depend upon composition, ionization balance and electron temperature at a physical radii of  $\sim 100 - 1000 R_*$ . Wind collisions in an interacting binary system will cause additional non-thermal (synchrotron) radio emission (Sect. 5.2), so care needs to be taken against overestimating mass-loss rates in this way.

Optical spectral lines observed in WR stars can be considered as recombination lines, although line formation is rather more complex in reality (Hillier 1988, 1989). Since recombination involves the combination of ion and electron density, the strength of wind lines scales with the square of the density. This explains why only a factor of  $\sim 10$  increase in wind density with respect to the photospheric absorption line spectrum from O supergiants produces an emission line Wolf-Rayet spectrum. Recall the comparison of  $\zeta$  Pup (O4I(n)f) to HD 96548 (WR40, WN8) in Figure 5.

### 4.3 Clumping

Evidence for highly clumped winds for WR and O stars, first detected in by Moffat et al. (1988), appears overwhelming. Line profiles show propagating small-scale structures or ‘blobs’, which are turbulent in nature (e.g. Moffat et al. 1988; Lépine et al. 2000). Wind structures have been investigated using radiation hydrodynamical simulations for optically thin lines by Dessart & Owocki

(2005). Individual spectral lines, formed at  $\sim 10R_*$  can be used to estimate (small) volume filling factors,  $f$  (Hillier 1991), from a comparison between line electron scattering wings (which scale linearly with density) and recombination lines (density-squared). This technique suffers from an approximate radial dependence and is imprecise due to severe line blending, especially in WC stars. Nevertheless,  $f \sim 0.05 - 0.25$  provide reasonable matches to observed line profiles, such that global WR mass-loss rates are reduced by a factor of  $\sim 2 - 4$  relative to homogeneous models.

Non-LTE model atmosphere spectroscopic fits to UV, optical and IR line profiles permit the determination of mass-loss rates and clumping filling factors, for which representative values are included in Table 2. Clumped mass-loss rates for Milky Way WN stars span a wide range of  $10^{-5.6}$  to  $10^{-4.4} M_\odot \text{ yr}^{-1}$ , with a much narrower range of  $10^{-5.0}$  to  $10^{-4.4} M_\odot \text{ yr}^{-1}$  for WC stars. Independent methods support clumped WR mass-loss rates, notably in binary systems using the variation of linear polarization as a function of orbital phase. The phase dependent modulation of linear polarization due to the relative motion of the companion originates via Thomson scattering of photons from the companion by the free electrons in the WR wind. This technique has been applied to several WR binaries including V444 Cyg (HD 193576=WR139, WN5+O) by St-Louis et al. (1993). This approach was developed further by Kurosawa, Hillier & Pittard (2002) using a 3D Monte Carlo approach, and supported a clumping factor of  $f \sim 0.06$  for V444 Cyg.

The most likely theoretical explanation for the structure in WR and O star winds is evidence for a strong instability of line driving in radiative winds – assuming that their winds are driven by radiation pressure – inducing small-

scale velocity perturbations (Lucy & Solomon 1971; Owocki, Castor & Rybicki 1988). There is a strong potential in line scattering to drive wind material with accelerations that greatly exceed the mean outward acceleration. Simulations demonstrate that this instability may lead naturally to a highly structured flow dominated by multiple shock compressions, producing X-rays in such regions, albeit relatively soft. Hard X-ray fluxes appear to be limited to colliding wind systems (e.g.  $\gamma$  Vel: Schild et al. 2004), for which  $10^{-7} \leq L_X/L_{\text{bol}} \leq 10^{-6}$ .

#### 4.4 Metallicity dependent winds?

Nugis, Crowther & Willis (1998) estimated clumping corrected mass-loss rates for Galactic WR stars from archival radio observations. These were coupled to parameters derived from spectroscopic analysis and/or evolutionary predictions to provide empirical mass-loss scaling relations (Nugis & Lamers 2000). For their combined sample, they obtained

$$\log \dot{M}/(M_{\odot} \text{yr}^{-1}) = -11.00 + 1.29 \log L/L_{\odot} + 1.74 \log Y + 0.47 \log Z \quad (6)$$

where Y and Z are the mass fractions of helium and metals, respectively. We shall now consider empirical evidence in favour of metallicity-dependent WR winds.

**4.4.1 WN WINDS** Smith & Willis (1983) compared the properties of LMC to Milky Way WN stars and concluded there was no significant differences between the two populations. These conclusions were supported by Hamann & Koesterke (2000) from detailed non-LTE modelling, although a large scatter in mass-loss rates within each parent galaxy was revealed. Either there is no metallicity dependence, or any differences are too subtle to be identified from the narrow metallicity range spanned by the Milky Way and LMC. Figure 7 compares the mass-loss rates of cluster or association member Milky Way WN3–6 stars with

LMC counterparts, as derived from their near-IR helium lines (following Howarth & Schmutz 1992), indicating stronger winds for stars without surface hydrogen. Indeed, Nugis & Lamers (2000) included the He content in their mass-loss prescription for WN stars (Eqn 6), which is broadly supported by recent results of Hamann, Gräfener & Liermann (2006). The substantial scatter in mass-loss rates is in line with the heterogeneity of line strengths within WN subtypes.

Comparison between H-rich WN3–6 stars in the Milky Way and Magellanic Clouds suggests an  $-0.4$  dex offset in mass-loss rates for the SMC ( $1/5 Z_{\odot}$ ) stars with respect to the Milky Way/LMC stars ( $1/2$  to  $1 Z_{\odot}$ ), i.e. a metallicity dependence of  $dM/dt \propto Z^m$  with  $m \sim 0.8 \pm 0.2$ , i.e. comparable to that for O stars (Mokiem et al. 2007). Within the Milky Way, most late-type stars contain hydrogen and most early-type stars do not, which is no longer true in the Magellanic Clouds (Smith, Shara & Moffat 1996; Foellmi, Moffat & Guerrero 2003ab) for which early-types dominate the WN populations (recall Figure 3).

There are two atmospheric factors contributing towards earlier WN subtypes at lower metallicities;

1. CNO compromises  $\sim 1.1\%$  by mass of the Solar photosphere (Asplund et al. 2004) versus  $0.48\%$  in the LMC and  $0.24\%$  in the SMC (Russell & Dopita 1990). Since WN stars typically exhibit CNO equilibrium abundances, there is a maximum nitrogen content available within a particular environment. Crowther (2000) demonstrated that for otherwise identical parameters – regardless of metallicity dependent mass-loss rates – a decreased nitrogen content at lower metallicity favours an earlier subtype, due to the respective abundance sensitivity of nitrogen classification lines
2. A metallicity dependence of WN winds would enhance the trend to earlier

spectral subtypes. High wind densities – at high metallicities – would lead to efficient recombination from high ionization stages (e.g.  $\text{N}^{5+}$ ) to lower ions (e.g.  $\text{N}^{3+}$ ), close to the optical line formation regions. This would not occur so readily for low density winds.

Consequently, both factors favour predominantly late subtypes at high metallicity, and early subtypes at low metallicity, which is indeed generally observed.

**4.4.2 WC WINDS** It is well established that WC stars in the inner Milky Way, and indeed all metal-rich environments, possess later spectral types than those in the outer Galaxy, LMC and other metal-poor environments (Figure 3). This observational trend towards earlier WC subtypes at lower metallicity, together with early recombination line studies of early WC stars, led Smith & Maeder (1991) to suggest that early WC stars are more carbon-rich than late WC stars. This has been widely adopted, but failed to be confirmed by quantitative analysis of WC subtypes (Koesterke & Hamann 1995).

What is the origin of the WC5–8 spectral type distribution in the Solar Neighbourhood versus the WC4 and WO subtypes in the LMC? Let us consider the WC classification lines – C III 5696 and C IV 5801–12 – in greater detail. Specifically the upper level of  $\lambda 5696$  has an alternative decay via  $\lambda 574$ , with a branching ratio of 147:1 (Hillier 1989). Consequently  $\lambda 5696$  only becomes strong when  $\lambda 574$  is optically thick, i.e. if the stellar temperature is low *or* the wind density is sufficiently high. From non-LTE models we have established that the temperatures of Galactic WC5–7 stars and LMC WC4 stars are similar, such that the observed subtype distribution argues that the wind densities of Galactic WC stars must be higher than the LMC stars.

Figure 7 also compares clumping corrected mass-loss rates of WC stars in the

Milky Way and LMC. The Galactic sample agree well with Eqn 6 from Nugis & Lamers (2000), whilst Crowther et al. (2002) obtain a similar dependence for LMC WC4 stars, albeit offset by  $-0.25$  dex, suggesting a dependence of  $dM/dt \propto Z^m$  with  $m \sim 0.6 \pm 0.2$ . Crowther et al. (2002) provided a basis for the different WC subtype distributions for the LMC and Milky Way, in the sense that all known LMC WC stars are WC4 stars (negligible C III  $\lambda 5696$  emission) whilst Solar Neighbourhood WC stars span WC5–9 (weak to strong C III  $\lambda 5696$  emission). This result followed from the fact that C III 5696Å emission is very sensitive to mass-loss rate, which in turn argues in favour of a metallicity dependence for WC winds.

#### 4.5 Line driving in WR winds

Historically, it has not been clear whether radiation pressure alone is sufficient to drive the high empirical mass-loss rates of WR stars. Let us briefly review the standard Castor, Abbott & Klein (1975, hereafter CAK) theory behind radiatively driven winds before addressing the question of line driving for WR stars. Pulsations have also been proposed for WR stars, as witnessed in intensive monitoring for the most photometrically variable WN8 star with the *MOST* satellite by Lefèvre et al. (2005). Interpretation of such observations however remains ambiguous (Townsend & MacDonald 2006; Dorfi, Gautschy & Saio 2006).

4.5.1 SINGLE SCATTERING LIMIT The combination of plentiful line opacity in the extreme UV, where the photospheric radiation originates, allows for efficient driving of hot star winds by radiation pressure (Milne 1926). In a static atmosphere, the photospheric radiation will only be efficiently absorbed or scattered in the lower layers of the atmosphere, weakening the radiative acceleration,

$g_{\text{line}}$ , in the outer layers. If the outer layers are expanding, the velocity gradient allows the atoms to see the photosphere as apparent red-shifted radiation. This Doppler shift allows atoms in the outer atmosphere to absorb undiminished continuum photons in their line transitions (Sobolev 1960).

The force from optically thick lines, which provide the radiative acceleration by absorbing the photon momentum, scale with the velocity gradient, such that there can be at most  $\approx c/v_\infty$  thick lines, implying a so-called single-scattering limit

$$\dot{M}v_\infty \leq L/c. \quad (7)$$

Castor, Abbott & Klein (1975) and Abbott (1982) developed a self-consistent solution of the wind properties, from which one obtains a velocity ‘law’

$$v(r) = v_\infty \left(1 - \frac{R_*}{r}\right)^\beta \quad (8)$$

for which  $\beta=0.8$  for O-type stars if the finite angular extent of the stellar disk is taken into account (Pauldrach, Puls & Kudritzki 1986).  $g_{\text{line}}$  can be written in terms of the electron scattering acceleration, i.e.  $g_{\text{line}} = g_e X(t)$  such that the equation of motion can be expressed as

$$v \frac{dv}{dr} = \frac{GM}{r^2} (\Gamma_e (1 + X(t)) - 1). \quad (9)$$

It is clear that both  $\Gamma_e$  and  $X(t)$  need to be large for a hot star to possess a wind. In the CAK approach, optically thick lines are assumed not to overlap within the wind. In fact, this is rarely true in the extreme UV where spectral lines are very tightly packed and the bulk of the line driving originates. Consequently, another approach is needed for WR stars whose winds exceed the single scattering limit (Lamers & Leitherer 1993). The critical parameter involving the development of strong WR winds is their proximity to the Eddington limit, according to Gräfener

& Hamann (2006).

**4.5.2 MULTIPLE SCATTERING** Since metal lines drive O star winds, empirically  $dM/dt \propto Z^m$ , with  $m \sim 0.8$  (Mokiem et al. 2007). Historically, the strength of WR winds were considered to be mass dependent, but metallicity-independent (Langer 1989). In Sect. 4.4 we have shown that there is evidence in favour of metallicity-dependent WR winds, with a sensitivity comparable to O stars, suggesting their winds are indeed radiatively driven.

Lucy & Abbott (1993) and Springmann (1994) produced Monte Carlo wind models for WR stars in which multiple-scattering was achieved by the presence of multiple ionization stages in the wind. However, a prescribed velocity and ionization structure was adopted in both case studies, plus the inner wind acceleration was not explained. Schmutz (1997) first tackled the problem of driving WR winds from radiatively driven winds consistently, i.e. limited wind driving in the deepest layers, plus the lack of force in the outer layers. Using a combined Monte Carlo and radiative transfer approach he introduced a means of photon loss from the He II Ly $\alpha$  303Å line via a Bowen resonance-fluorescence mechanism (involving overlapping Ca V, Fe VI and O III lines), leading to a change in the ionization equilibrium of helium, and resulting in a higher stellar luminosity. Photon loss nevertheless failed to initiate a sufficiently powerful acceleration in the deep atmospheric layers, whilst the inclusion of clumping by Schmutz (1997) did succeed in maintaining a self-consistent strong outflow in the outer wind. Subsequent studies have supported the principal behind the photon loss mechanism for WR stars, although the effect is modest (e.g. De Marco et al. 2000). Similar outer wind results were obtained by e.g. Herald et al. (2001).

The next advance for the inner wind driving was by Nugis & Lamers (2002)

whose analytical study suggested that the (hot) iron opacity peak at  $10^{5.2}\text{K}$  is responsible for the observed WR mass-loss in an optically thick wind (a cooler opacity peak exists at  $10^{4.6}\text{K}$ ). Indeed, the line-driving from opacities of highly ionized Fe ions (Fe IX-XVII) provided the first self-consistent inner wind solution by Gräfener & Hamann (2005) for WR111 (HD 165763=WR111, WC5), i.e. the wind acceleration due to radiation and gas pressure matches the mechanical and gravitational acceleration. Gräfener & Hamann (2005) achieved the observed terminal wind velocity via an extreme outer wind clumping filling factor of  $f=0.02$ , which is unrealistic since predicted line electron scattering wings are too weak with respect to observations. The inclusion of more complete opacities from other elements such as Ne and Ar should permit a more physical outer wind solution. The velocity structure from their hydrodynamical model closely matches a typical  $\beta=1$  velocity law of the form in Eqn 8 in the inner wind, versus a slower  $\beta=5$  law in the outer wind, for which the hybrid velocity structure proposed by Hillier & Miller (1999) produced a reasonable match.

Theoretically, both the hydrodynamical models of Gräfener & Hamann (2005, 2006) and recent Monte Carlo wind models for WR stars by Vink & de Koter (2005) argue in favour of radiation pressure through metal lines as responsible for the multiple scattering observed in WR stars. The latter study – for WR stars with fixed stellar temperatures and Eddington parameters – suggests a metallicity scaling for WN subtypes, i.e.  $dM/dt \propto Z^m$  with  $m=0.86$  for  $10^{-3} \leq Z/Z_{\odot} \leq 1$ , which is similar to O stars (Mokiem et al. 2007). Gräfener & Hamann (2006) demonstrated that the exponent decreases for late-type WN stars at higher  $\Gamma_e$ , such that a more complex dependence is necessary, and also predict reduced wind velocities at lower metallicity. Vink & de Koter (2005) propose that the higher

metal content of WC atmospheres suggests a weaker dependence with exponent  $m=0.66$  for  $10^{-1} \leq Z/Z_{\odot} \leq 1$  and  $m=0.35$  for  $10^{-3} \leq Z/Z_{\odot} \leq 10^{-1}$ . Further observational studies of WR stars spanning a broad a range of metallicities are necessary to ensure current theoretical predictions are indeed appropriate.

## 5 Interacting Binaries

### 5.1 Close binary evolution

The components of a massive binary may evolve independently, as if they were single stars for sufficiently large orbital periods. Alternatively, the more massive component in a binary will expand to fill its Roche lobe, and the binary becomes an interacting or close binary, with mass exchange from the primary to the secondary. For an initial period of several days, the primary will reach its Roche lobe whilst still on the H-core burning main sequence (Case A) and transfer the majority of its hydrogen rich envelope to the secondary, resulting in a He burning WR primary with a secondary on the main-sequence that has now increased in mass. For longer periods, of order weeks, mass transfer will occur during the hydrogen-shell burning phase (Case B), or during He-shell burning (Case C) for initial periods of several years. Cases B and C are much more common than Case A due to the much larger range of orbital periods sampled, although a common envelope will occur instead of Roche lobe overflow if there is an LBV phase according to Vanbeveren, De Loore & Van Rensbergen (1998).

Relative to single star evolution, close binary evolution will extend the formation of WR stars to lower initial mass, and consequently lower luminosity (e.g. Vanbeveren et al. 1998). The observed lower limit to WR formation in the Milky Way is broadly consistent with the single star case (Meynet & Maeder 2003), so

either low-mass He stars are not recognised spectroscopically as WR stars due to reduced wind strength, or they may be too heavily diluted by their brighter O star companions for them to be observed.

One natural, albeit rare, consequence of massive close binary evolution involves the evolution of the initial primary to core-collapse, with a neutron star or black hole remnant, in which the system remains bound as a high mass X-ray binary (HMXB, Wellstein & Langer 1999). The OB secondary may then evolve through to the Wolf-Rayet phase, producing a WR plus neutron star or black hole binary. For many years, searches for such systems proved elusive, until it was discovered that Cyg X-3, a 4.8h binary possessed the near-IR spectrum of a He-star (van Kerkwijk et al. 1992). Nevertheless, the nature of Cyg X-3 remains somewhat controversial.

## 5.2 Colliding winds

The presence of two early-type stars with stellar winds within a binary system naturally leads to a wind interaction region. In general, details of the interaction process are investigated by complex hydrodynamics, although an analytical approach following Stevens, Blondin & Pollock (1992) provides a useful insight into the physics of the colliding winds.

A subset of WR stars display non-thermal (synchrotron) radio emission, in addition to the thermal radio emission produced via free-free emission from the stellar wind. This indicates that a magnetic field must be present in the winds of such stars, and that relativistic electrons exist in the radio emitting region. Shocks associated with a wind collision may act as sites for particle acceleration through the Fermi mechanism (Eichler & Usov 1993), in which case free electrons

would undergo acceleration to relativistic velocities by crossing the shock front. The majority of non-thermal WR radio emitters are known binaries. For example, WR140 (WC7+O) is a highly eccentric system, for which the radio flux is thermal over the majority of the orbit. However, between phases 0.55 and 0.95 (where phase 0 corresponds to periastron passage), the radio flux increases dramatically and displays a non-thermal radio index. As a result of the cavity produced by the shock cone in the WR wind, the non-thermal radio emission can reach us when the O star passes in front of the WR star (Williams et al. 1990).

One may introduce the wind momentum ratio,  $R$

$$R = \frac{\dot{M}_1 v_{\infty,1}}{\dot{M}_2 v_{\infty,2}} \quad (10)$$

where the mass loss rates and wind velocities of components  $i$  are given by  $\dot{M}_i$  and  $v_{\infty,i}$ , respectively. In the simplest case of  $R=1$ , the intersection between the winds occurs in a plane midway between the two stars. In the more likely situation of  $R \neq 1$ , the contact discontinuity appears as a cone wrapped around the star with the less momentum in its wind. As an example, radio emission in the WR147 (WN8 + B0.5) system has been resolved into two components: thermal emission from the WN8 primary wind, plus non-thermal emission located close to the companion (Williams et al. 1997). The location of the non-thermal component is consistent with the ram pressure balance of the two stellar winds, as expected in a colliding wind system from which a momentum ratio of  $R \sim 0.011$  can be obtained.

For early-type stars that have reached their terminal velocities of several thousand  $\text{km s}^{-1}$ , the post-shock plasma temperature is very high ( $\geq 10^7 \text{ K}$ ), such that the main signature of shock-heated plasma is anticipated in X-rays, such that one expects significantly stronger X-ray luminosity from massive binaries,

as a function of the bolometric luminosity, plus phase-locked modulation. The latter is expected either from the changing opacity along the line-of-sight or changing separation in eccentric binaries (Stevens, Blondin & Pollock 1992).  $\gamma$  Vel (WC8+O) is one such colliding wind binary for which *ROSAT* X-ray observations revealed substantial phase-locked variability. The X-ray emission from the shock is absorbed when the opaque wind from the WR star is in front, but becomes significantly less absorbed at orbital phases when the cavity around the O star crosses the line-of-sight (Willis, Schild & Stevens 1995).

### 5.3 Dust formation

The principal sources of interstellar dust are cool, high mass-losing stars, such as red giants, asymptotic giant branch stars, plus novae and supernovae. Dust is observed around some massive stars, particularly LBVs with ejecta nebulae, but aside from their giant eruptions, this may be material that has been swept up by the stellar wind. The intense radiation fields of young, massive stars ought to prevent dust formation in their local environment. However, Allen, Swings & Harvey (1972) identified excess IR emission, due to heated circumstellar dust in a subset of WC stars, of which some form dust persistently, whilst others are episodic.

Williams, van der Hucht & Thé (1987) investigated the infrared properties of dusty Galactic WC stars, and highlighted the difficulty of forming and maintaining dust in such a harsh environment, for which grain temperatures of  $\sim 1000\text{K}$  have been derived. The challenge is how to generate sufficient neutral carbon sufficiently close to the WC star in order to form grains. Assuming homogeneity and spherical symmetry, carbon is predicted to remain singly or even doubly ionized

due to high electron temperatures of  $\sim 10^4$  K in the region where dust formation is observed to occur. A clue to the origin of dust is provided by WR140 (WC7+O) which forms dust episodically, close to periastron passage, where the power in the colliding winds from each star is at its greatest (Williams et al. 1990). Usov (1991) demonstrated analytically that the wind conditions of WR140 at periastron favour a strong gas compression in the vicinity of the shock surface, such that there is a strong outflow of cold gas. Whilst this does not explain how the grains can form, it provides a much more amenable environment, i.e. high density, low temperature, carbon-rich material associated with the bow-shock between the stellar winds.

If binarity is responsible for the episodic subclass, what is the situation for the persistent dust makers, such as WR104? Conclusive proof of the binary nature of WR104 has been established by Tuthill, Monnier & Danchi (1999) from high spatial resolution near-IR imaging. Dust associated with WR104 forms a spatially confined stream that follows a spiral trajectory (so-called ‘pinwheel’), analogous to a garden rotary sprinker. The cocoon stars after which the Quintuplet cluster at the Galactic Centre was named have recently been identified as dusty WC pinwheel stars by Tuthill et al. (2006).

Binarity appears to play a key role in the formation of dust in WC stars, providing the necessary high density within the shocked wind interaction region, plus shielding from the hard ionizing photons, such that all dust formers may be binaries. However, not all WC binaries form dust (e.g.  $\gamma$  Vel). The presence of hydrogen from the OB companion may provide the necessary chemical seeding in the otherwise H-free WC environment, although even this possibility has its difficulties, since chemical mixing between the WC and OB winds may not occur

in the immediate vicinity of the shock region.

## 6 Evolutionary models and properties at core-collapse

The various inputs to stellar interior evolutionary models originate from either laboratory experiments (e.g. opacities, nuclear reaction rates) or astronomical observations (e.g. mass-loss properties, rotation rates). Indeed, mass-loss (rather than convection) has a dominant effect upon stellar models for the most massive stars. One example of this approach – illustrating the potential pitfalls – is as follows. According to Koesterke et al. (1991), stellar luminosities of some weak-lined early-type WN stars were unexpectedly low ( $\leq 10^5 L_\odot$ ). In order to reproduce such results, plus the observed N(WR)/N(O) ratio, Meynet et al. (1994) adopted higher mass-loss rates, relative to previous empirical calibrations. Subsequent improvements in non-LTE WR models have led to higher luminosities (e.g. Hamann, Gräfener & Liermann 2006), and so removed the need for elevated mass-loss rates. Indeed, allowance for clumping has led to reduced, rather than enhanced, mass-loss rates in atmospheric models.

### 6.1 Rotational mixing

Mass-loss and rotation are intimately linked for the evolution of massive stars, in which stellar winds will lead to spin-down for the case of an efficient internal angular momentum transport mechanism. Since metallicity impacts upon the strength of stellar winds, the spin-down of massive stars is anticipated to be rapid at Solar metallicity (Langer 1998). Consequently, initial rotational velocity properties are erased within a few million years, except in metal-poor environments where initial conditions may remain preserved throughout the main sequence lifetime

of O-type stars due to weak stellar winds. For massive O stars with high initial rotation rates, the surface velocity may increase as a result of the transport of angular momentum by meridional circulation (Maeder & Meynet 2001).

Various deficiencies in certain non-rotating evolutionary models – including the existence of intermediate WN/C stars (though see Langer 1991), plus the observed WR population at low metallicity – led to the incorporation of rotational mixing into recent models following the theoretical treatment of Zahn (1992). Rotational mixing reproduces some of the properties from the high mass-loss models of Meynet et al. (1994), for which two approaches have been developed. Meynet & Maeder (1997) describe the transport of angular momentum in the stellar interior through the shear and meridional instabilities. Alternatively, Heger et al. (2000) include magnetic fields such that the redistribution of angular momentum in the stellar interior during core H-burning is close to rigid rotation, such that momentum is transported radially from the core to the surface. Since magnetic fields of neutron stars (magnetars) are of order  $10^{12}$  G ( $10^{15}$  G), one would expect a field of  $10^2$  G ( $10^3$  G) for their progenitor Wolf-Rayet stars, for which the first observational limits are becoming available, namely  $\leq 25$  G for HD 50896 (WR6, St-Louis et al. 2006).

Rotation favours the evolution into the WR phase at earlier stages, adding to the WR lifetime, plus allowing lower initial mass stars to go through a WR phase, i.e. reducing the initial mass from  $37M_{\odot}$  ( $v_{\text{rot}}=0$  km s $^{-1}$ ) to  $22M_{\odot}$  ( $v_{\text{rot}}=300$  km s $^{-1}$ ) at Solar metallicity (Meynet & Maeder 2003). Initial rotation velocities have been studied for the young SMC cluster NGC 346, whose weak OB winds would not be expected to cause significant loss of angular momentum, for which  $v_{\text{rot}} \sim 175 \pm 125$  km s $^{-1}$  (Mokiem et al. 2006), suggesting somewhat lower initial

rotation rates, on average. Nevertheless, lower mass limits for the formation of WR stars as a function of metallicity are predicted to lie in the range  $42M_{\odot}$  at  $Z=0.004$  (SMC) to  $21M_{\odot}$  at  $Z=0.04$  (M 83) for models allowing for such high initial rotation rates (Meynet & Maeder 2005). Hirschi, Meynet & Maeder (2005) present chemical yields from rotating stellar models at Solar metallicity, revealing increased C and O yields below  $30M_{\odot}$ , and higher He yields at higher initial masses.

## 6.2 Evolutionary model predictions

For regions of constant star formation (as opposed to starbursts), representative of Local Group galaxies, one can estimate a theoretical number ratio of WR to O stars from their average lifetimes, weighted over the Initial Mass Function (IMF). For an assumed Salpeter IMF slope for massive stars, the ratios obtained by rotating evolutionary models are in much better agreement with the observed WR to O star number ratio at Solar metallicity (Meynet & Maeder 2003). However, since the O star population is relatively imprecise, the observed WR subtype distributions are often used instead.

From Figure 3, the Solar Neighbourhood WR subtype distribution contains similar numbers of WC and WN stars, with an equal breakdown between early (H-free) and late (H-rich) WN stars. From comparison with evolutionary models, the agreement is reasonable, except for the brevity of the H-deficient WN phase in interior models at Solar metallicity. This aspect has been quantified by Hamann, Gräfener & Liermann (2006) who calculated synthetic WR populations from the Meynet & Maeder (2003) evolutionary tracks assuming a standard Salpeter IMF. The synthetic sample predicts that only 20% of WN stars should

be hydrogen-free, in contrast to over 50% of the observed sample. Non-rotating models provide better statistics, although low luminosity early-type WN stars are absent in such synthetic populations. The poor agreement between the low luminosity of synthetic late-type WN stars and high spectroscopic luminosities relies, in part, upon the choice of absolute magnitude–spectral type calibration.

The ratio of WC to WN stars increases with increasing metallicity for nearby galaxies whose WR content has been studied in detail, as illustrated in Figure 8. A notably exception is the low metallicity Local Group galaxy IC 10 (Massey & Holmes 2002; Crowther et al. 2003). However, the WR population of IC 10 remains controversial, since high Galactic foreground extinction favours the detection of WC stars over WN stars, owing to the equivalent widths of the strongest optical lines in WC stars being (up to 100 times) larger than those of the strongest optical lines in WN stars (Massey & Johnson 1998). Two evolutionary model predictions are included in Fig. 8, either allowing for rotation during its evolution, but without a WR metallicity scaling (Meynet & Maeder 2005), or neglecting rotation but with a WR metallicity scaling (Eldridge & Vink 2006). The latter models, in which convective overshooting is included, agree much better at medium to high metallicities. Similar calculations including binary evolution were considered by Van Bever & Vanbeveren (2003). Consequently, whilst rotating evolutionary models for single stars – incorporating contemporary mass-loss rate prescriptions – resolve many issues with respect to earlier comparisons to observations, problems persist. Notably, the Solar Neighbourhood WN subtype distribution, and high metallicity WC to WN ratio disagree with predictions.

In very metal-poor environments ( $\sim 1/50 Z_{\odot}$ ) the WR phase is predicted for only the most massive single stars ( $\geq 90M_{\odot}$ ) according to non-rotating models

of de Mello et al. (1998). WR stars are observed in UV and optical spectroscopy of such metal-poor regions within I Zw 18 (Izotov et al. 1997; Brown et al. 2002) and SBS 0335-052E (Papaderos et al. 2006). Only WC stars have been unambiguously identified spectroscopically, yet WN stars are expected to dominate the WR population.

Line strength of winds from WN stars are believed to depend more sensitively upon metallicity than WC stars (Vink & de Koter 2005), such that WN stars may be extremely difficult to directly detect in such metal-poor galaxies. Hot, weak-lined WN stars are predicted to have hard ionizing flux distributions, they may be indirectly indicated via the presence of strong nebular He II 4686 emission, which is indeed strong in I Zw 18, SBS 0335-052E and other very metal-poor star forming galaxies. Depending upon the exact wind dependence upon metallicity, potentially large WR populations are inferred in such galaxies (Crowther & Hadfield 2006), which single star evolutionary models have difficulty in reproducing. Close binary evolution may represent the primary formation channel for such metal-poor WR stars, unless LBV eruptions provide the dominant method of removing the H-rich envelope at low metallicity.

### 6.3 WR stars as SNe and GRB progenitors

The end states of massive stars have been studied from a theoretical perspective by Heger et al. (2003). In particular, WN and WC stars are the likely progenitors of (at least some) Type Ib and Type Ic core-collapse SN, respectively, since H and H+He are weak/absent in such SNe (Woosley & Bloom 2006). Empirical evidence connecting single WR stars to Type Ib/c SN is presently lacking, for which lower mass interacting binaries represent alternative progenitors. Since WR lifetimes

are a few  $10^5$  yr (Meynet & Maeder 2005), one would need observations of  $\geq 10^4$  WR stars in order to firmly establish a connection on a time frame of a few years. Hadfield et al. (2005) identified  $10^3$  WR stars in M83, such that similar narrow-band optical surveys of a dozen other high star forming spiral galaxies within  $\sim 10$  Mpc, would likely provide the necessary statistics, albeit hindered by low spatial resolution from ground-based observations.

Nevertheless, the light curves of two famous Type Ic supernovae – SN 1998bw and SN 2003dh – indicate ejected core masses of order  $10\text{--}12 M_\odot$  (Nakamura et al. 2001; Mazzali et al. 2003), which agree rather well with the masses of LMC WC4 stars inferred by Crowther et al. (2002), if we additionally consider several solar masses which remain as a compact (black hole) remnant. Both these supernovae were associated with long GRBs, namely 980425 (Galama et al. 1998) and 030329 (Hjorth et al. 2003), supporting the ‘collapsar’ model (MacFadyen & Woosley 1999). WR populations have been detected in the host galaxy of GRB 980425, albeit offset from the location of the GRB by several hundred pc (Hammer et al. 2006), suggesting GRBs may be produced by runaway WR stars, ejected from high density star clusters (see, however, Fruchter et al. 2006).

The challenge faced by both single and binary evolutionary models is for a rotating core at the point of core-collapse (Woosley & Heger 2006). Single star models indicate that stars efficiently spin-down during either the slowly rotating RSG stage – due to the magnetic dynamo produced by differential rotation between the rotating He-core and non-rotating H-envelope – or the mechanical loss of angular momentum from the core during the high mass-loss WR phase. Indeed, spectropolarimetry does not favour rapid rotation for Milky Way WC stars, whilst some WN stars may possess significant rotation rates. Initial rapid

rotation of a single massive star may be capable of circumventing an extended envelope via chemically homogeneous evolution (Maeder 1987) if mixing occurs faster than the chemical gradients from nuclear fusion. At sufficiently low metallicity, mechanical mass-loss during the WR phase would be sufficiently weak to prevent loss of significant angular momentum permitting the necessary conditions for a GRB (Yoon & Langer 2005).

Alternatively, close binary evolution could cause the progenitor to spin-up due to tidal interactions or the merger of a black hole and He core within a common envelope evolution (Podsiadlowski et al. 2004). Both single and binary scenarios may operate, although the former is presently favoured since long-soft GRBs are predominantly observed in host galaxies which are fainter, more irregular and more metal deficient than hosts of typical core-collapse supernovae (e.g. Fruchter et al. 2006).

Of course, the ejecta strongly interacts with the circumstellar material, probing the immediate vicinity of the GRB itself (van Marle, Langer & García-Segura 2005). This provides information on the progenitor, for which one expects  $\rho \propto r^{-2}$  for WR winds (Eqn 4). The apparent metallicity-dependent WR winds argue that one would potentially expect rather different environments for the afterglows of long-duration GRBs, that were dependent upon the metallicity of the host galaxy. Indeed, densities of the immediate environment of many GRBs suggest values rather lower than typical Solar metallicity WR winds (Chevalier, Li & Frasson 2004). Fryer, Rockefeller & Young (2006) estimate half of long GRBs apparently occur in uniform environments, favouring a post-common envelope binary merger model.

## 7 Summary Points

1. The agreement between multi-wavelength spectroscopic observations of WR stars and current non-LTE model atmospheres is impressive, from which H-rich (core H-burning) WN stars may be distinguished from classic H-deficient (core He-burning) WN, WC and WO stars. In addition, significant progress has been achieved in interior evolutionary models through the incorporation of rotational mixing, such that the use of contemporary (i.e. low) mass-loss rates reproduce many of the observed properties of WR stars, at least those close to Solar metallicity.
2. Both empirical and theoretical evidence now favour metallicity-dependent WR winds. These provide a natural explanation of the WC (and WO) subtype distribution in different regions of the Milky Way and in external galaxies. A metallicity dependence is partially responsible for the WN subtype dependence, although the reduced nitrogen content in metal-poor galaxies also contributes. Further, the development of consistent radiatively driven WR winds represent an important milestone. The predicted metallicity dependence of mass-loss rates in radiatively driven wind models agrees with observations to date.
3. Overall, the apparent convergence of spectroscopic and interior models suggests that the role of WR stars to the ionizing, mechanical and chemical enrichment of the ISM has increased (due to higher luminosities from line blanketing), decreased (due to clumping) and increased (due to longer WC phases from rotational mixing) with respect to the previous Annual Review article on this subject (Abbott & Conti 1987).

## 8 Future Issues to be Resolved

1. Current non-LTE models rely upon an overly simplified clumpy wind structure and spherical symmetry. Theoretical hydrodynamic predictions for the radial dependence of clumping in WR winds is anticipated to represent a major area of development over the next decade together with two dimensional non-LTE radiative transfer codes.
2. Discrepancies persist between empirical WR populations and predictions from evolutionary models which allow for rotational mixing. Metallicity dependent WR winds may improve consistency, or allowance for magnetic fields. Spatially resolved clusters rich in WR stars, such as Westerlund 1 (if co-eval), provide a direct means of testing evolutionary predictions for co-eval stellar population, whilst observational limits on magnetic fields within Wolf-Rayet stars are underway.
3. The role of rotation in WR stars at low metallicity is of particular interest. At present, amongst the best means of establishing rapid rotation in WR stars is by measuring departures from spherical symmetry using spectropolarimetry, which has thus far been applied to bright WR stars in the Milky Way.
4. The evolutionary paths leading to WR stars and core-collapse SN remain uncertain, as is the role played by LBV eruptions for the most massive stars. Given the observational connection between Type Ic supernovae and long-soft GRBs, do the latter result from low metallicity massive stars undergoing chemically homogeneous evolution, massive binaries during a common envelope phase or runaways from dense star clusters?

5. The presence of WR stars in large numbers within very low metallicity galaxies appears contrary to the expectations of single star evolutionary models neglecting rotational mixing. Are such stars exclusively produced by close binary evolution, or via giant LBV eruptions?
6. Although most late WC stars are known to be dust formers, the universal presence of a binary companion is not yet established. In addition, it is not clear how dust grains form within such a harsh environment and merits further study.

### Acknowledgement

Thanks to Götz Gräfener, John Hillier, Norbert Langer, Georges Meynet, Tony Moffat, Nathan Smith, Dany Vanbeveren and Peredur Williams for useful comments on an early version of the manuscript. I wish to thank the Royal Society for providing financial assistance through their wonderful University Research Fellowship scheme for the past eight years.

### Key Terms

**Interference filter techniques:** WR candidates identified from narrow-band images sensitive to light from strong WR emission lines, after subtraction of images from adjacent continua

**P Cygni profiles:** Blue-shifted absorption plus red-shifted emission, characteristic of stellar outflows, associated with resonance transitions of abundant ions (e.g. C IV 1548-51Å).

**Non-LTE:** Solution of full rate equations is necessary due to intense radiation field, such that radiative processes dominate over collisional processes, i.e. the

LTE approximation is no longer valid.

**Radiatively driven winds:** The transfer of photon momentum in the photosphere to the stellar atmosphere through absorption by (primarily) metal spectral lines.

**Monte Carlo models:** Powerful statistical approach, using photon packets which undergo line scatterings.

**Clumped winds:** Radiatively driven winds are intrinsically unstable, producing compressions and rarefactions in their outflows.

**Collapsar model:** Rapidly rotating WR star undergoes core-collapse to form a black hole fed by an accretion disk, whose rotational axis collimates the GRB jet.

**Magnetar:** Highly magnetized neutron star, observationally connected with Soft Gamma Repeaters and Anomalous X-ray Pulsars.

## Reference Annotations

**Grafener & Hamann:** First solution of hydrodynamics within a realistic Wolf-Rayet model atmosphere.

**Hillier** Describes the extended atmospheric structure of a WC star.

**van der Hucht** Catalogue of Milky Way WR stars, including cluster membership, binarity, masses.

**Lamers et al.** Summary of key observational evidence in favour of a late stage of evolution for WR stars.

**Meynet & Maeder** Comparison between observed WR populations in galaxies with evolutionary model predictions allowing for rotational mixing.

**Schaerer & Vacca** Describes the determination of WR and O star populations

within unresolved galaxies.

**Williams et al.** Describes all aspects of dust formation around WC stars.

## Acronyms List

**GRB** Gamma Ray Burst

**LBV** Luminous Blue Variable

**RSG** Red Supergiant

**WN** Nitrogen sequence Wolf-Rayet

**WC** Carbon sequence Wolf-Rayet

**WO** Oxygen sequence Wolf-Rayet

**LTE** Local Thermodynamic Equilibrium

**IMF** Initial Mass Function

## Side Bar

Luminous Blue Variables, also known as Hubble-Sandage or S Doradus type variables, share many characteristics of Wolf-Rayet stars, and are widely believed to be the immediate progenitors of classic WN stars. They also possess powerful stellar winds, hydrogen depleted atmospheres such that similar analysis techniques may be used (e.g. Hillier et al. 2001). They occupy a part of the Hertzsprung-Russell diagram adjacent to Wolf-Rayet stars, with typical spectral morphologies varying irregularly between A-type (at visual maximum) and B-type (at visual minimum) supergiants. Examples include AG Car and P Cyg in the Milky Way, and S Dor and R127 in the LMC (e.g. Humphreys & Davidson 1994). Occasional eruptive events – signatures of which are circumstellar nebulae – most notably undergone by  $\eta$  Car during two decades in the 19th Century ( $\geq 10M_{\odot}$  ejected)

are believed to play a major role in the evolution of very massive stars via the removal of their hydrogen-rich envelope (Davidson & Humphreys 1997; Smith et al. 2003). The origin of such huge eruptions is unclear, since line-driven radiation pressure is incapable of producing such outflows.

#### LITERATURE CITED

Abbott DC, 1982. ApJ 263:723

Abbott DC, Bieging JH, Churchwell E, Torres AV. 1986. ApJ 303:239

Abbott DC, Conti PS. 1987. ARA&A 25:113

Abbott DC, Lucy LB. 1985. ApJ 288:679

Allen DA, Swings JP, Harvey PM. 1972. A&A 20:333

Anderson LS. 1989. ApJ 339:558

Asplund M, Grevesse N, Sauval AJ, Allende Prieto C, Kiselman D. 2004. A&A 417:751

Barlow MJ, Roche PF, Aitken DA. 1988. MNRAS 232:821

Barniske A, Hamann W-R, Gräfener G. 2006. In *Stellar Evolution at Low Metallicity: Mass-loss, Explosions, Cosmology*, ed. HJGLM Lamers, N Langer, T Nugis, San Francisco: ASP Conf Series in press

Bartzakos P, Moffat AFJ, Niemela VS. 2001. MNRAS 324:18

Beals CS. 1940. JRASC 34:169

Bohannan B, Walborn NR. 1989. PASP 101:520

Breysacher J, Azzopardi M, Testor G. 1999. A&AS 137:117

Brown TM, Heap SR, Hubeny I, Lanz T, Lindler D. 2002. ApJ 579:L75

Castor JI, Abbott DC, Klein RI. 1975. ApJ 195:157

Chevalier RA, Li Z-Y, Fransson C. 2004. ApJ 606:369

Chu Y-H, Treffers RR, Kwitter KB. 1983. *ApJS* 53:937

Clark JS, Negueruela I, Crowther PA, Goodwin SP. 2005. *A&A* 434:949

Conti PS, 1976, In *Proc. 20th Colloq. Int. Ap. Liége*, Liége: University of Liége, p. 193

Conti PS, Garmany CD, Massey P. 1989. *ApJ* 341:113

Conti PS, Garmany CD, De Loore C, Vanbeveren D. 1983. *ApJ* 274:302

Conti PS, Leep ME, Perry DN. 1983. *ApJ* 268:228

Conti PS, Massey P. 1989. *ApJ* 337:251

Conti PS, Massey P, Vreux J-M. 1990. *ApJ* 354:359

Crowther PA. 2000. *A&A* 356:191

Crowther PA. 2006. In *Stellar Evolution at Low Metallicity: Mass-loss, Explosions, Cosmology* eds. HJGLM Lamers, N Langer, T Nugis, San Francisco: ASP Conf Series in press (astro-ph/0510063)

Crowther PA, De Marco O, Barlow MJ. 1998. *MNRAS* 296:367

Crowther PA, Dessart L. 1998. *MNRAS* 296:622

Crowther PA, Dessart L, Hillier DJ, Abbott JB, Fullerton AW. 2002. *A&A* 392:653

Crowther PA, Drissen L, Abbott JB, Royer P, Smartt SJ. 2003. *A&A* 404:483

Crowther PA, Fullerton AW, Hillier DJ, Brownsberger K, Dessart L, et al. 2000. *ApJ* 538:L51

Crowther PA, Hadfield LJ. 2006. *A&A* 449:711

Crowther PA, Hadfield LJ, Clark JS, Negueruela I, Vacca WD. 2006b. *MNRAS* in press (astro-ph/0608356)

Crowther PA, Morris PW, Smith JD. 2006a. *ApJ* 636:1033

Crowther PA, Pasquali A, De Marco O, Schmutz W, Hillier DJ, de Koter A.

1999. A&A 350:1007

Crowther PA, Smith LJ. 1997. A&A 320:500

Crowther PA, Smith LJ, Hillier DJ. 1995b. A&A 302:457

Crowther PA, Smith LJ, Hillier DJ, Schmutz W. 1995a. A&A 293:427

Crowther PA, Smith LJ, Willis AJ. 1995c. A&A 304:269

Davidson K, Humphreys RM. 1997. ARA&A 35:1

de Koter A, Schmutz W, Lamers HJGLM. 1993. A&A 277:561

De Marco O, Schmutz W, Crowther PA, Hillier DJ, Dessart L, et al. 2000. A&A 358:187

de Mello DF, Schaerer D, Heldmann J, Leitherer C. 1998. ApJ 507:199

Dessart L, Crowther PA, Hillier DJ, Willis AJ, Morris PW, van der Hucht KA. 2000. MNRAS 315:407

Dessart L, Owocki SR. 2005. A&A 432:281

Dopita MA, Bell JF, Chu Y-H, Lozinskaya TA. 1994. ApJS 93:455

Dorfi EA, Gautschy A, Saio H. 2006. A&A 453:L35

Drew JE, Barlow MJ, Unruh YC, Parker QA, Wesson R, et al. 2004, MNRAS 351:206

Eenens PRJ, Williams PM. 1994. MNRAS 269:1082

Eichler D, Usov V. 1993. ApJ 402:271

Eldridge JJ, Vink JS. 2006. A&A 452:295

Esteban C, Smith LJ, Vilchez JM, Clegg RES. 1993. A&A 272:299

Evans CJ, Howarth ID, Irwin MJ, Burnley AW, Harries TJ. 2004. MNRAS 353:601

Figer DF. 2005. Nat 434:192

Foellmi C, Moffat AFJ, Guerrero MA. 2003a. MNRAS 338:360

Foellmi C, Moffat AFJ, Guerrero MA. 2003b. MNRAS 338:1025

Fruchter AS, Levan AJ, Strolger L, Vreeswijk PM, Thorsett SE, et al. 2006. Nat 441:463

Fryer CL, Rockefeller G, Young PA. 2006. ApJ. 647:1269

Galama TJ, Groot PJ, van Paradijs J, Kouveliotou C, Augusteijn T, et al. 1998. Nat 395:670

Gal-Yam A, Leonard DC, Fox DB, Cenko SB, Soderberg AM, et al. ApJ submitted (astro-ph/0608029)

Gamov G. 1943. ApJ 98:500

Garnett DR, Kennicutt RCJr, Chu Y-H, Skillmann ED. 1991. PASP 103:850

**Gräfener G, Hamann W-R. 2005. A&A 432:633**

Gräfener G, Hamann W-R. 2006. A&A submitted

Gräfener G, Koesterke L, Hamann W-R. 2002. A&A 387:244

García-Segura G, Langer N, MacLow M-M. 1996b. A&A 316:133

García-Segura G, MacLow M-M, Langer N. 1996a. A&A 305:229

Gonzalez Delgado RM, Leitherer C, Stasinska G., Heckman TM. 2002. ApJ 580:824

Hadfield LJ, Crowther PA. 2006. MNRAS 368:1822

Hadfield LJ, Crowther PA, Schild H, Schmutz W. 2005. A&A 439:265

Hadfield LJ, Van Dyk S, Morris PW, Smith JD, Marston AP. 2007 MNRAS submitted

Hamann W-R, Dunnebeil G, Koesterke L, Wessolowski U, Schmutz W. 1991. A&A 249:443

Hamann W-R, Gräfener G. 2004. A&A 427:697

Hamann W-R, Gräfener G, Liermann A. 2006. A&A 457:1015

Hamann W-R, Koesterke L. 2000. A&A 360:647

Hamann W-R, Koesterke L, Wessolowski U. 1993. A&A 274:397

Hammer F, Flores H, Schaefer D, Dessauges-Zavadsky M, Le Floch E, Puech M. 2006. A&A 454:103

Harries TJ, Hillier DJ, Howarth ID. 1998. MNRAS 296:1072

Heger A, Langer N, Woosley SE. 2000. ApJ 528:368

Heger A, Fryer CL, Woosley SE, Langer N, Hartmann DH. 2003. ApJ 591:288

Herald JE, Hillier DJ, Schulte-Ladbeck RE. 2001. ApJ 548, 932

Hillier DJ. 1987. ApJS 63:947

Hillier DJ. 1988. ApJ 327:822

**Hillier DJ. 1989. ApJ 347:392**

Hillier DJ. 1991. A&A 247:455

Hillier DJ, Miller DL. 1998. ApJ 496:407

Hillier DJ, Miller DL. 1999. ApJ 519:354

Hillier DJ, Davidson K, Ishibashi K, Gull T. 2001. ApJ 553:837

Hiltner WA, Schild RE. 1966. ApJ 143:770

Hirschi R, Meynet G, Maeder A. 2005. A&A 433:1013

Hjorth J, Sollerman J, Moller P, Fynbo JPU, Woosley SE, et al. 2003. Nat 423:847

Homeier N, Blum RD, Pasquali A, Conti PS, Damineli A. 2003. A&A 408:153

Howarth ID, Schmutz W. 1992. A&A 261:503

Humphreys RM, Davidson K. 1979. ApJ 232:409

Humphreys RM, Davidson K. 1994. PASP 106:1025

Izotov YI, Foltz CB, Green RF, Guseva NG, Thuan TX. 1997. ApJ 487:L37

Kingsburgh RL, Barlow MJ. 1995. A&A 295:171

Kingsburgh RL, Barlow MJ, Storey PJ. 1995. A&A 295:75

Koesterke L, Hamann W-R. 1995. A&A 299:503

Koesterke L, Hamann W-R, Schmutz W, Wessoloski U. 1991. A&A 248:166

Kudritzki RP, Puls J. 2000. ARA&A 38:613

Kurosawa R, Hillier DJ, Pittard JM. 2002. A&A 388:957

Kurosawa R, Hillier DJ, Schulte-Ladbeck RE. 1999. AJ 118:539

Lamers HJGLM, Leitherer C. 1993. ApJ 412:771

**Lamers HJGLM, Maeder A, Schmutz W, Cassinelli JP. 1991. ApJ 368:538**

Lamontagne R, Moffat AFJ, Drissen L, Robert C, Matthews JM. 1996, AJ 112:2227

Langer N. 1989. A&A 220:135

Langer N. 1991. A&A 248:531

Langer N. 1998. A&A 329:551

Langer N, Hamann W-R, Lennon M, Najarro F, Paoldrach AWA, Puls J. 1994. A&A 290:819

Lefévre L, Marchenko SV, Moffat AFJ, Chené AN, Smith SR, et al. 2005. ApJ 634:L109

Leitherer C, Chapman JM, Koribalski B. 1997. ApJ 481:898

Lépine S, Moffat AFJ, St-Louis N, Marchenko SV, Dalton MJ et al. 2000, AJ 120:3201

Levesque EM, Massey P, Olsen KAG, Plez B, Josselin E, Maeder A, Meynet G. 2005. ApJ 628:973

Lucy LB, Abbott DC. 1993. ApJ 405:738

MacFadyen AI, Woosley SE. 1999. ApJ 524:262

Maeder A. 1987 A&A 178, 159

Maeder A, Meynet G. 1994. A&A 287:803

Maeder A, Meynet G. 2001. A&A 373:555

Marchenko SV, Moffat AFJ, Crowther PA, Chené A-N, De Serres M, et al. 2004. MNRAS 353:153

Martins F, Schaerer D, Hillier DJ. 2002. A&A 382:999

Massey P. 1980. ApJ 236:526

Massey P. 1984. ApJ 281:789

Massey P. 2002. ApJS 141:81

Massey P. 2003. ARA&A 41:15

Massey P, Armandroff TE, Conti PS. 1986. AJ 92:1303

Massey P, Conti PS. 1981. ApJ 244:173

Massey P, DeGioia-Eastwood K, Waterhouse E. 2001. AJ 121:1050

Massey P, Holmes S. 2002. ApJ 580:L35

Massey P, Johnson O. 1998. ApJ 505:793

Massey P, Olsen KAG, Parker JWm. 2003. AJ 126:2362

Massey P, Parker JWm, Garmány CD. 1989. AJ 98:1305

Mazzali PA, Deng J, Tominaga N, Maeda K, Nomoto K, et al. 2003. ApJ 599:L95

Meynet G, Maeder A. 1997. A&A 321:465

Meynet G, Maeder A. 2003. A&A 404:975

**Meynet G, Maeder A. 2005. A&A 429:581**

Meynet G, Maeder A, Schaller G, Schaerer D, Charbonnel C. 1994. A&AS 103:97

Milne EA. 1926. MNRAS 86:459

Moffat AFJ, Drissen L, Lamontagne R, Robert C. 1988. ApJ 334:1038

Moffat AFJ, Seggewiss W, Shara MM. 1985. ApJ 295:109

Moffat AFJ, Shara MM. 1987. ApJ 320:266

Mokiem MR, De Koter A, Evans CJ, Puls J, Smartt SJ et al. 2006. *A&A* 456:1131

Mokiem MR, De Koter A, Vink J, Puls J, Evans CJ et al. 2007. submitted

Morris PM, Crowther PA, Houck JR. 2004. *ApJS* 154:413

Morton DC. 1967. *ApJ* 147:1017

Nakamura T, Mazzali PA, Nomoto K, Iwamoto K. 2001. *ApJ* 550:991

Nugis T, Crowther PA, Willis AJ. 1998. *A&A* 333:956

Nugis T, Lamers HJGLM. 2000. *A&A* 360:227

Nugis T, Lamers HJGLM. 2002. *A&A* 389:162

Owocki SR, Castor JI, Rybicki GB. 1988. *ApJ* 355:914

Owocki SR, Cranmer SR, Gayley KG. 1996. *ApJ* 472:L115

Papaderos P., Izotov YI, Guseva NG, Thuan TX, Fricke KJ. 2006. *A&A* 454:119

Pauldrach AWA, Puls J, Kudritzki RP. 1986. *A&A* 184:86

Petrovic J, Pols O, Langer N. 2006. *A&A* 450:219

Podskadlowski Ph, Langer N, Poelarends AJT, Rappaport S, Heger A, Pfahl E. 2004. *ApJ* 612:1044

Prinja RK, Barlow MJ, Howarth ID. 1990. *ApJ* 361:607

Rauw G, Crowther PA, De Becker M, Gosset E, Naze Y, et al. 2005. *A&A* 432:985

Repolust T, Puls J, Herrero A. 2004. *A&A* 415:349

Russell SC, Dopita MA. 1990. *ApJS* 74:93

Schaerer D, Maeder A. 1992. *A&A* 263:129

Schaerer D, Contini T, Pindao M. 1999. *A&AS* 136:35

**Schaerer D, Vacca, WD. 1998. *ApJ* 497:618**

Schild H, Crowther PA, Abbott JB, Schmutz W. 2003. *A&A* 397:859

Schild H, Güdel M, Mewe R, Schmutz W, Raassen AJJ, et al. 2004. *A&A* 422:177

Schild H, Maeder A. 1984. *A&A* 136:237

Schmutz W. 1997. A&A 321:268

Schmutz W, Hamann W-R, Wessolowski U. 1989. A&A 210:236

Schmutz W, Leitherer C, Gruenwald R. 1992. PASP 104:1164

Schweickhardt J, Schmutz W, Stahl O, Szeifert Th, Wolf B. 1999. A&A 347:127

Shapley AE, Steidel CS, Pettini M., Adelberger KL. 2003. ApJ 588:65

Skinner SL, Zhekov SA, Güdel M, Schmutz W. 2002. ApJ 579:764

Smith LF. 1968a. MNRAS 138:109

Smith LF. 1968b. MNRAS 140:409

Smith LF, Hummer DG. 1988. MNRAS 230:511

Smith LF, Maeder A. 1991. A&A 241:77

Smith LF, Shara MM, Moffat AFJ. 1996. MNRAS 281:163

Smith LJ, Crowther PA, Prinja RK. 1994. A&A 281:833

Smith LJ, Norris RPF, Crowther PA. 2002. MNRAS 337:1309

Smith LJ, Willis AJ. 1983. A&AS 54:229

Smith N, Gehrz RD, Hinz PM, Hoffmann WF, Hora JL, et al. 2003 AJ 125:1458

Smith N, Owocki SP. 2006. ApJ 645:L45

Sobolev VV. 1960. *Moving Envelopes of Stars*, Cambridge, Mass: Harvard University Press

Springmann U. 1994. A&A 289:505

Stahl O, Wolf B, Klare G, Cassatella A, Krautter J. et al. 1983. A&A 127:49

Stevens IR, Blondin JM, Pollock AMT. 1992. ApJ 386:265

St-Louis N, Moffat AFJ, Lapointe L, Efimov YS, Shakhovskoj NM, Fox GK, Pirola V. 1993. ApJ 410:342

St-Louis N, Chene, A-N, de la Chevrotiere A, Moffat AFJ. 2006. In *Mass loss from stars and the evolution of stellar clusters*, ed. A de Koter, LJ Smith, R

Waters, San Francisco: ASP Conf Ser, in press

Torres AV, Conti PS, Massey P. 1986. ApJ 300:379

Torres-Dodgen AV, Massey P. 1988. AJ 96:1076

Townsend RHD, MacDonald J. 2006. MNRAS 368:L57

Turner DG, 1982. In *IAU Symp 99: Wolf-Rayet Stars: Observations, Physics, Evolution*, ed. CWH de Loore, AJ Willis, Reidel: Dordrecht, p.57

Tuthill PG, Monnier JD, Danchi WC. 1999. Nat 398:487

Tuthill P, Monnier J, Tanner A, Figer D, Ghez A, Danchi W. 2006. Sci 313:935

Usov VV. 1991. MNRAS 252:49

Vacca WD, Rayner RJ, Cushing MC. 2006. ApJ submitted

Van Bever J., Vanbeveren D. 2003. A&A 400:63

Vanbeveren D, De Loore C, Van Rensbergen W. 1998. A&A Rev 9:63

**van der Hucht KA. 2001. New A 45:135**

van der Hucht KA. 2006. A&A 458, 453

van der Hucht KA, Morris PW, Williams PM, Setia Gunawan DY. 1996. A&A 315:L193

van Kerkwijk MH, Charles PA, Geballe TR, King DL, Miley GK, et al. 1992. Nat 355:703

van Marle AJ, Langer N, García-Segura G. 2005. A&A 444:837

Villar-Sbaffi A, St-Louis N, Moffat AFJ, Piironen V. 2006. ApJ 640:995

Vink JS, de Koter A. 2005. A&A 442:587

Von Zeipel H. 1924. MNRAS 84:665

Walborn NR. 1990, in *Properties of Hot, Luminous Stars*, ed. CD. Garmany, San Francisco: ASP Conf Ser 7, p.23

Walborn NR, Morrell NI, Howarth ID, Crowther PA, Lennon DJ, et al. 2004.

ApJ 608:1028

Weaver R, McCray R, Castor JI, Shapiro P, Moore R. 1977. ApJ 218:377

Wellstein S, Langer N. 1999 A&A. 350:148

Westerlund BE. 1966. ApJ 145:724

Williams PM, Dougherty SM, Davis RJ, van der Hucht KA, Bode MF, Setia  
Gunawan DY. 1997. MNRAS 289:10

Williams PM, van der Hucht KA, Pollock AMT, Florkowski DR, van der Woerd  
H, Wamsteker WM. 1990. MNRAS 243:662

**Williams PM, van der Hucht KA, Thé PS. 1987. A&A 182:91**

Willis AJ, Crowther PA, Fullerton AW, Hutchings JB, Sonneborn G, et al. 2004.  
ApJS 154:651

Willis AJ, Schild H, Stevens IR. 1995. A&A 298:549

Willis AJ, van der Hucht KA, Conti PS, Garmany CD. 1986. A&AS 63:417

Wolf CJE, Rayet G. 1867. Comptes Rendues 65:292

Woosley SE, Bloom JS. 2006. ARA&A 44:507

Woosley SE, Heger A. 2006. ApJ 637, 914

Wright AE, Barlow MJ. 1975. MNRAS 170:41

Yoon S-C, Langer N. 2005. A&A 443:643

Zahn J-P. 1992. A&A 265:115

Table 1: Wavelength specific observed and synthetic spectral atlases (X-ray to mid-IR) of Galactic WR stars, including the predicted luminosity in each spectral band for late and early subtypes, based upon the averages of HD 96548 (WR40, WN8, Herald, Hillier & Schulte-Ladbeck 2001), HD 164270 (WR103, WC9, Crowther, Morris & Smith 2006a) and HD 50896 (WR6, WN4b, Morris, Crowther & Houck 2004), HD 37026 (BAT52, WC4, Crowther et al. 2002), respectively.

$\lambda$	Window	$L/L_{\text{bol}}$		Sp Type	Ref
		Late	Early		
5–25Å	X-ray	$10^{-7}$	$10^{-7}$	WN	Skinner et al. 2002
				WC	Schild et al. 2004
<912Å	Extreme UV	39%	69%	WN, WC	Smith, Crowther & Norris 2000
				WN	Hamann & Gräfener 2004
912–1200Å	Far-UV	21%	12%	WN, WC	Willis et al. 2004
1200–3200Å	UV, Near-UV	33%	16%	WN, WC	Willis et al. 1986
3200–7000Å	Visual	5%	2%	WN, WC	Conti & Massey 1989
7000–1.1μm	Far-red	0.9%	0.3%	WN, WC	Conti, Massey & Vreux 1990
				WN, WC	Howarth & Schmutz 1992
1–5μm	Near-IR	0.4%	0.2%	WN, WC	Vacca et al. 2006
5–30μm	Mid-IR	0.02%	0.01%	WN	Morris et al. 2000
				WCd	van der Hucht et al. 1996

Table 2: Physical and wind properties of Milky Way WR stars (LMC in parenthesis), adapted from Herald, Hillier & Schulte-Ladbeck (2001) and Hamann, Gräfener & Liermann (2006) for WN stars, plus Barniske, Hamann & Gräfener (2006), Crowther et al. (2002, 2006a) and references therein for WC stars. Abundances are shown by mass fraction in percent. Mass-loss rates assume a volume filling factor of  $f=0.1$ .

Sp	$T_*$	$\log L$	$\dot{M}$	$v_\infty$	$\log N(\text{LyC})$	$M_v$	Example
Type	kK	$L_\odot$	$M_\odot \text{yr}^{-1}$	$\text{km s}^{-1}$	$\text{ph s}^{-1}$	mag	
WN stars							
3-w	85	5.34	-5.3	2200	49.2	-3.1	WR3
4-s	85	5.3	-4.9	1800	49.2	-4.0	WR6
5-w	60	5.2	-5.2	1500	49.0	-4.0	WR61
6-s	70	5.2	-4.8	1800	49.1	-4.1	WR134
7	50	5.54	-4.8	1300	49.4	-5.4	WR84
8	45	5.38	-4.7	1000	49.1	-5.5	WR40
9	32	5.7	-4.8	700	48.9	-6.7	WR105
WNha stars							
6ha	45	6.18	-5.0	2500	49.9	-6.8	WR24
9ha	35	5.86	-4.8	1300	49.4	-7.1	WR108
WC and WO stars							
(WO)	(150)	(5.22)	(-5.0)	(4100)	(49.0)	(-2.8)	(BAT123)
(4)	(90)	(5.54)	(-4.6)	(2750)	(49.4)	(-4.5)	(BAT52)
5	85	5.1	-4.9	2200	48.9	-3.6	WR111
6	80	5.06	-4.9	2200	48.9	-3.6	WR154
7	75	5.34	-4.7	2200	49.1	-4.5	WR90
8	65	5.14	-5.0	1700	49.0	-4.0	WR135
9	50	4.94	-5.0	1200	48.6	-4.6	WR103

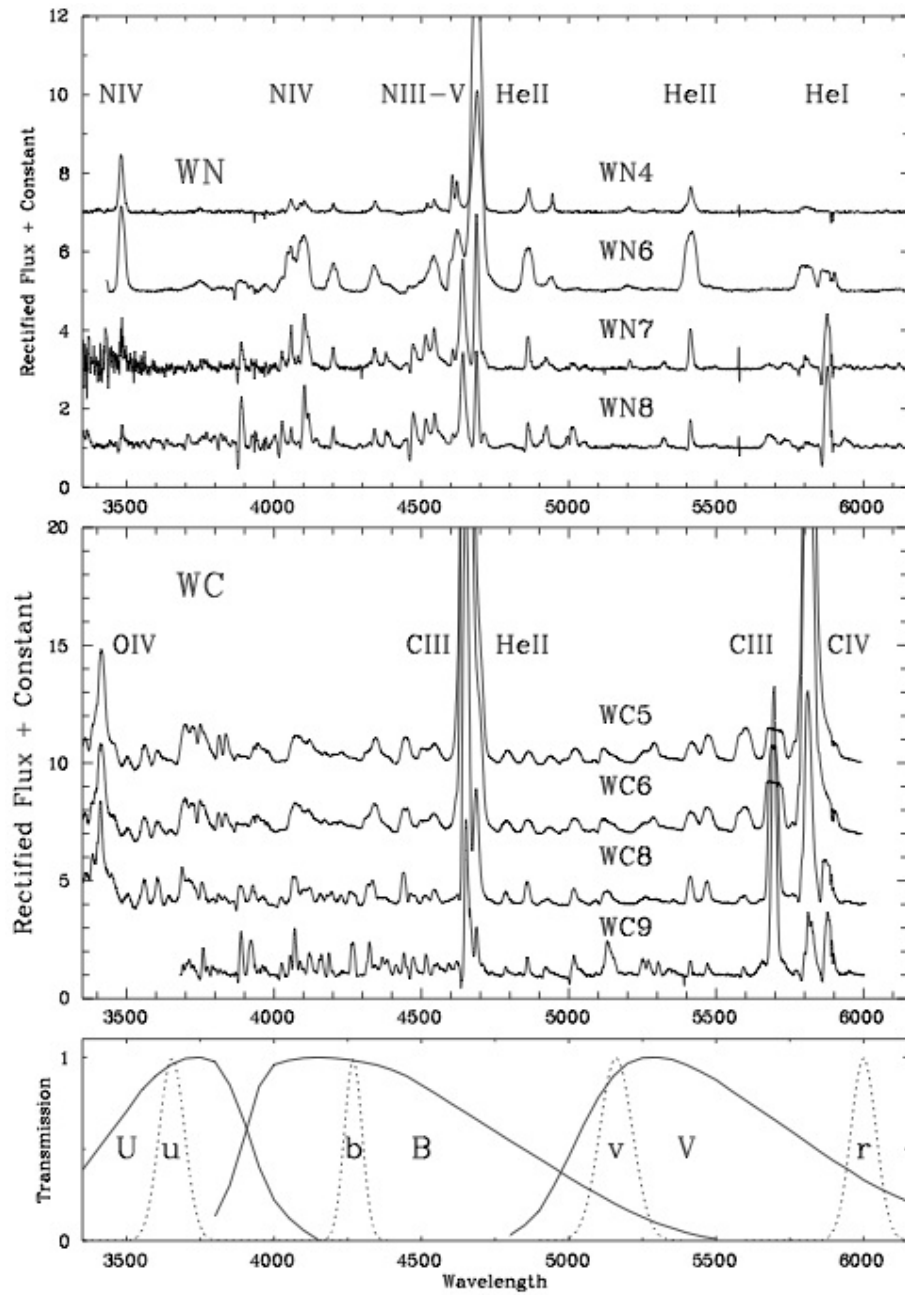


Figure 1: Montage of optical spectroscopy of Milky Way WN and WC stars together with the Smith (1968b) *ubv* and Massey (1984) *r* narrow-band and Johnson UBV broad-band filters

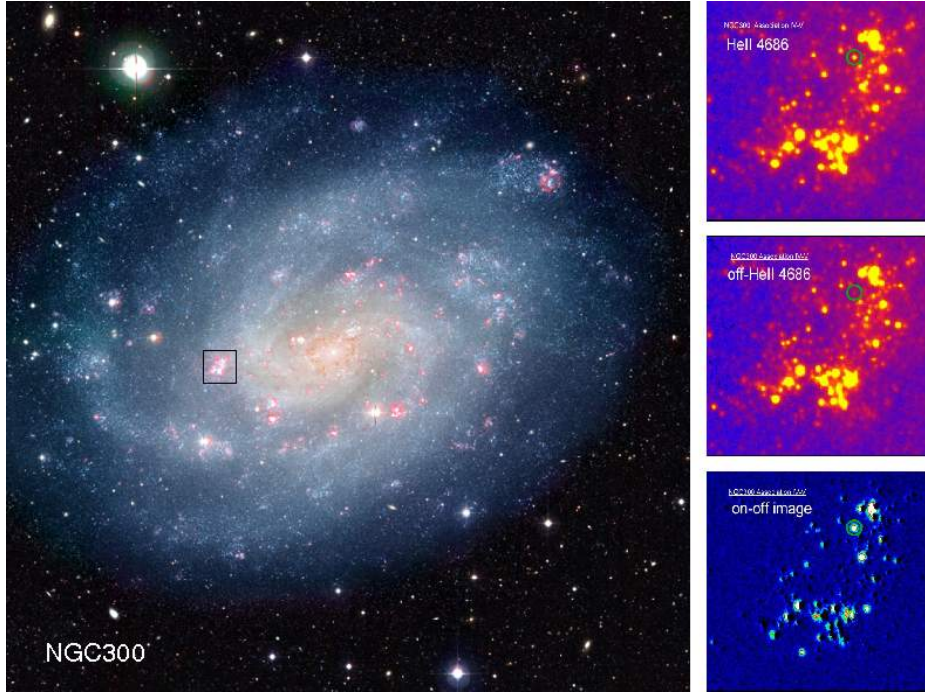


Figure 2: Composite ESO Wide Field Imager B, V, R and H $\alpha$  image of NGC 300 obtained at the MPG/ESO 2.2m telescope (Press Photo 18a-h/02), with the OB association IV-V indicated (40 $\times$ 40 arcsec), together with narrow-band images of the association centred at  $\lambda$ 4684 (on-He II 4686, top) and  $\lambda$ 4781 (off-He II 4686, middle), and a difference image (on-off, bottom) obtained with ESO VLT/FORS2 (Schild et al. 2003). A number of WR stars showing a He II excess (white) can be seen in the lower image, including a WC4 star (green circle in all FORS2 images).

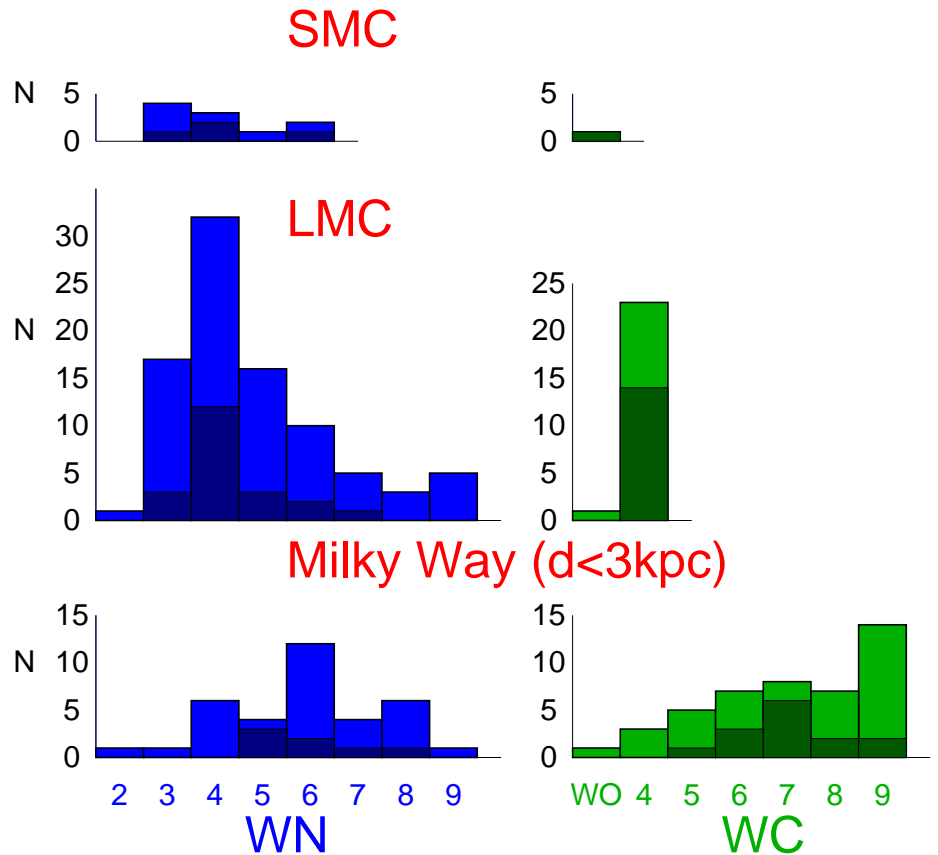


Figure 3: Subtype distribution of Milky Way ( $d < 3\text{kpc}$ ), LMC and SMC WR stars, according to van der Hucht (2001), Bartzakos, Moffat & Niemela (2001), Foellmi, Moffat & Guerrero (2003ab) in which both visual and close WR binaries are shaded (e.g. only 3 of the LMC WC4 stars are close binaries according to Bartzakos et al. 2001). Rare, intermediate WN/C stars are included in the WN sample.

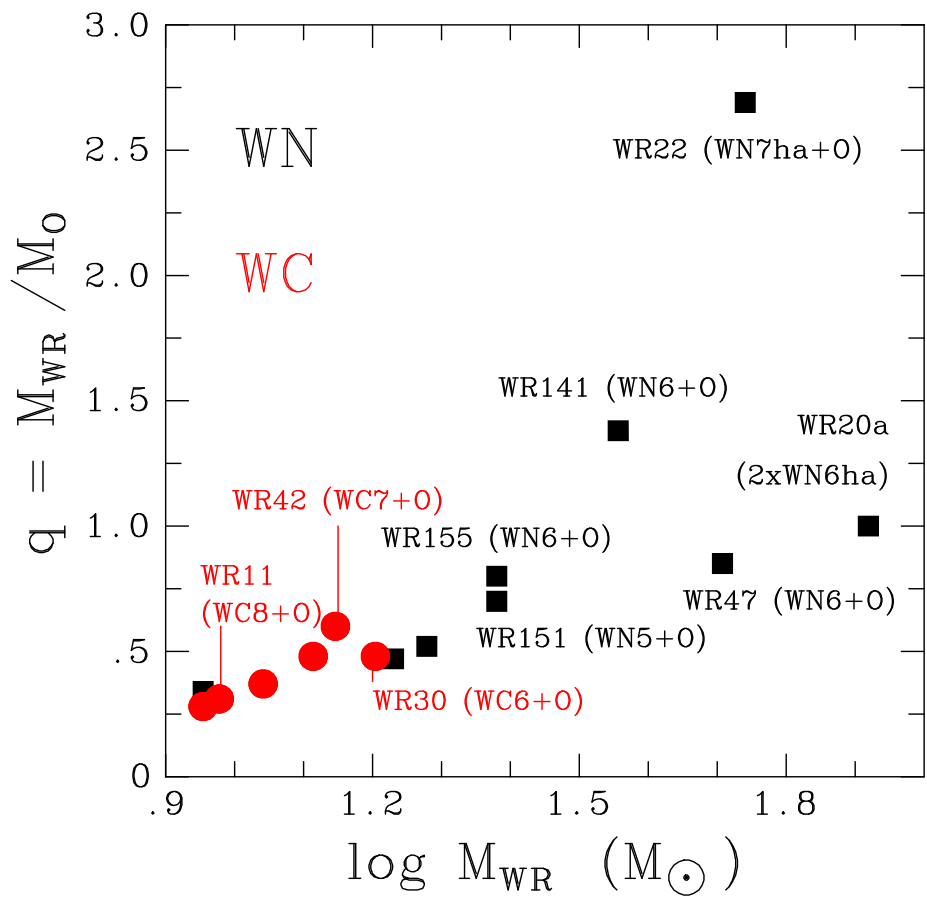


Figure 4: Stellar masses for Milky Way WR stars obtained from binary orbits  
(van der Hucht 2001; Rauw et al. 2005; Villar-Sbaffi et al. 2006)

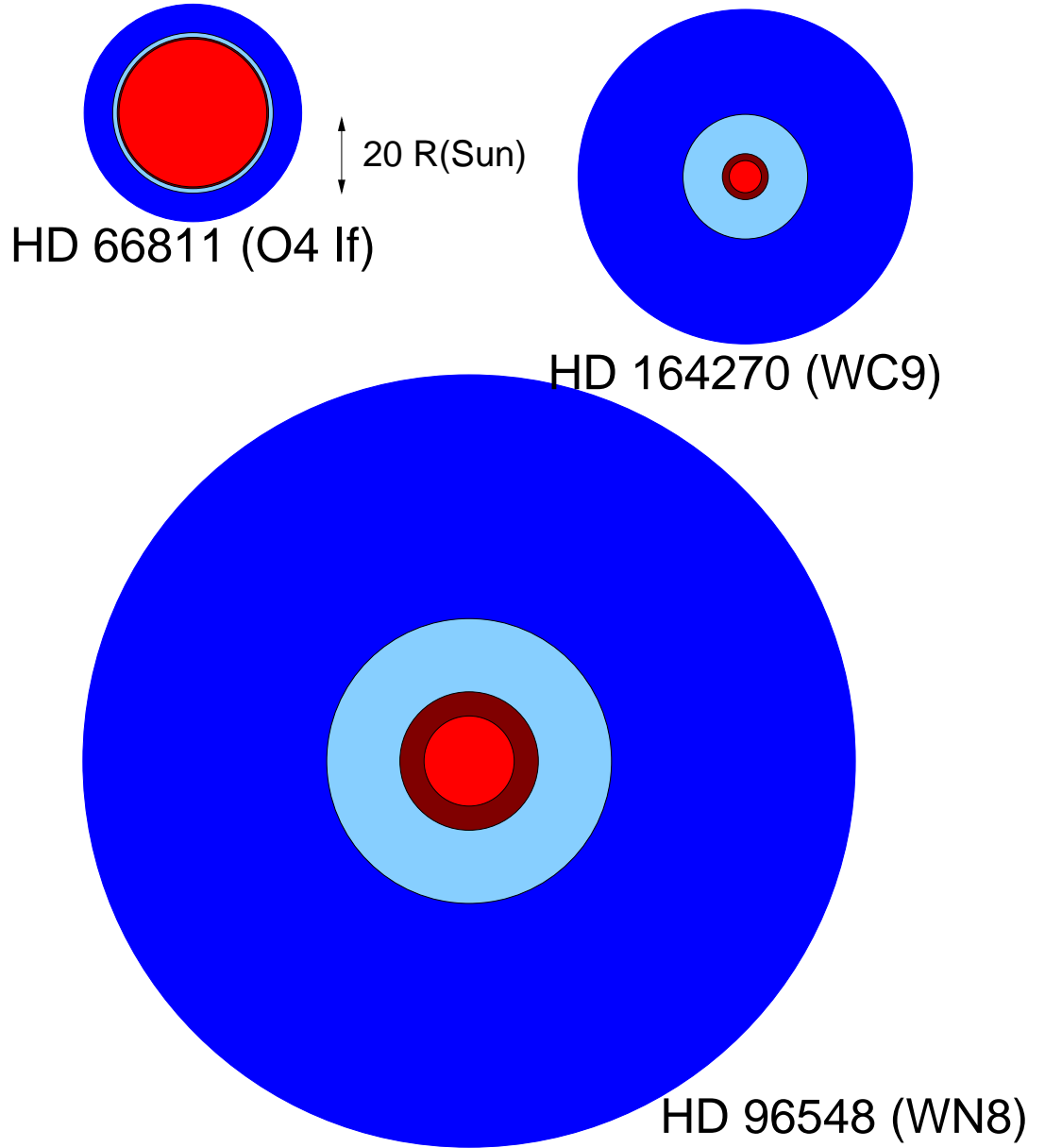


Figure 5: Comparisons between stellar radii at Rosseland optical depths of 20 ( $= R_*$ , red) and  $2/3$  ( $= R_{2/3}$ , dark red) for HD 66811 (O4 If), HD 96548 (WR40, WN8) and HD 164270 (WR103, WC9), shown to scale, together with the region corresponding to the primary optical wind line forming region,  $10^{11} \leq n_e \leq 10^{12} \text{ cm}^{-3}$  (dark blue), plus  $n_e \geq 10^{12} \text{ cm}^{-3}$  (light blue) in each case, illustrating the highly extended winds of WR stars with respect to O stars (Repolust, Puls & Herrero 2004; Herald, Hillier & Schulte-Ladbeck 2001; Crowther, Morris & Smith 2006a).

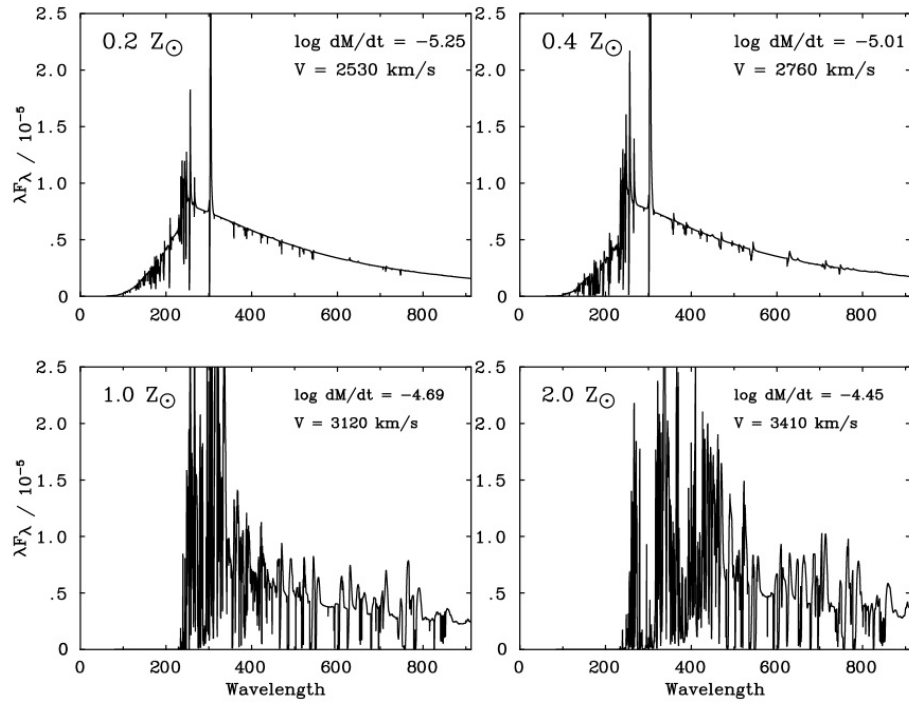


Figure 6: Comparison between the Lyman continuum ionizing fluxes of early WN CMFGEN models with fixed parameters (100kK,  $\log L/L_\odot = 5.48$ ), except that the mass-loss rates and wind velocities depend upon metallicities according to Smith, Norris & Crowther (2002), such that solely the low wind density models predict a significant flux below the  $\text{He}^+$  edge at 228Å

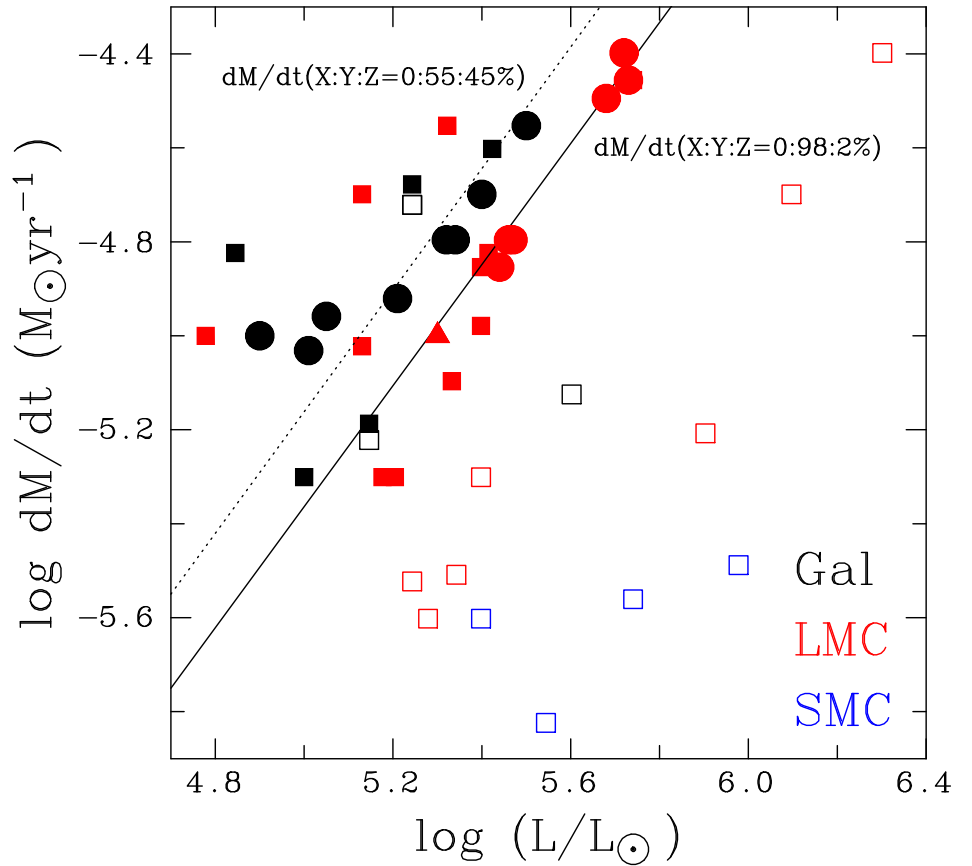


Figure 7: Comparison between the mass-loss rates and luminosities of WN3-6 (squares), WC5-9 (circles) and WO (triangles) stars in the Galaxy (black), LMC (red) and SMC (blue). We include Eqn 6 from Nugis & Lamers (2000) for H-poor WN (solid line) and WC stars (dotted line). Open/filled symbols refer to WN stars with/without surface hydrogen, based upon analysis of near-IR helium lines (Crowther 2006). Mass-loss rates are universally high if hydrogen is absent.

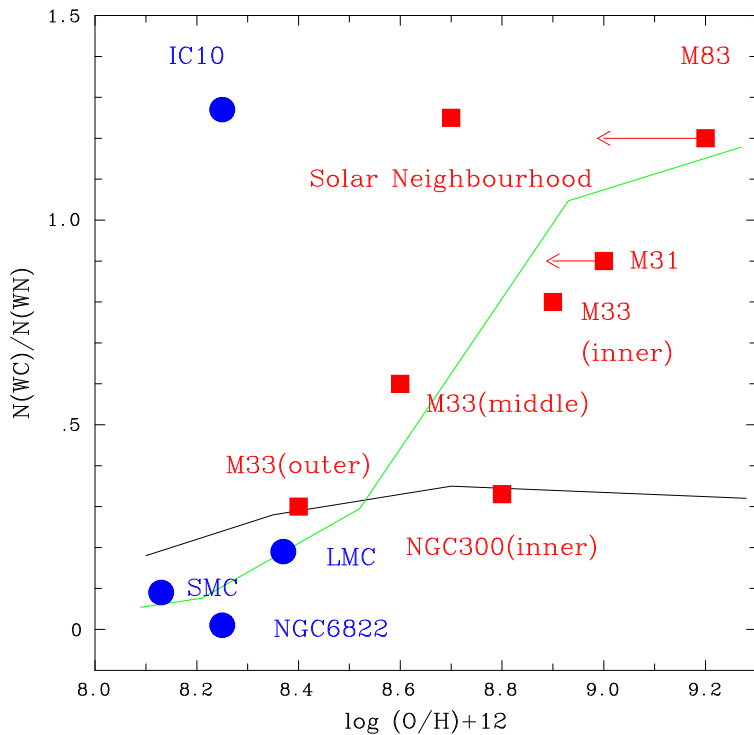


Figure 8: Comparison between observed  $N(WC)/N(WN)$  ratio and oxygen content, for nearby spiral (red) and irregular (blue) galaxies (Massey & Johnson 1998; Crowther et al. 2003; Schild et al. 2003; Hadfield et al. 2005) together with evolutionary model predictions by Meynet & Maeder (2005, black) and Eldridge & Vink (2006, green)